Constraining dark energy

V.Ruhlmann-Kleider
CEA/Irfu/DPhP - Saclay

1) State of the art, Type Ia supernovae (SNe Ia)
2) **Baryonic acoustic oscillations (BAO) and beyond (RSD)**
3) Weak lensing (WL)
4) The H_0 tension

Baryonic acoustic oscillations

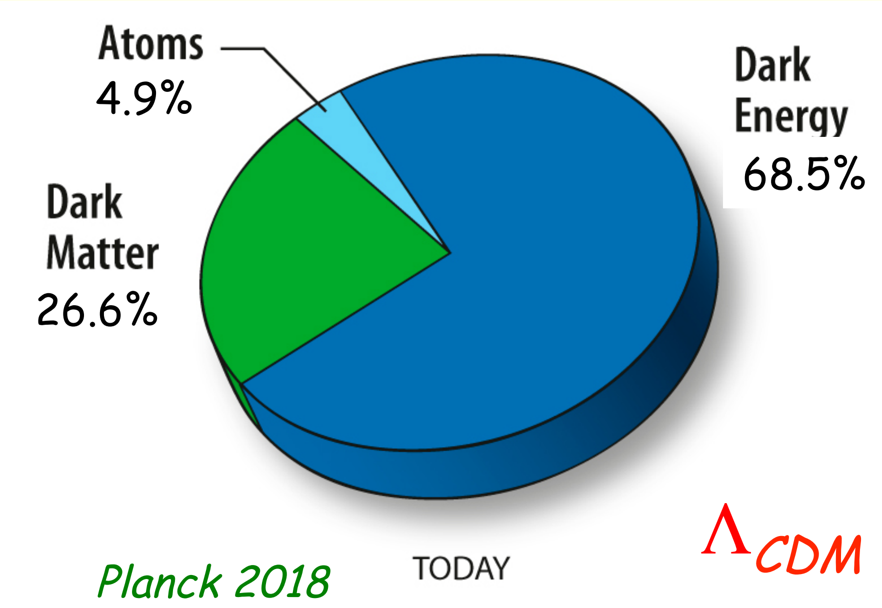

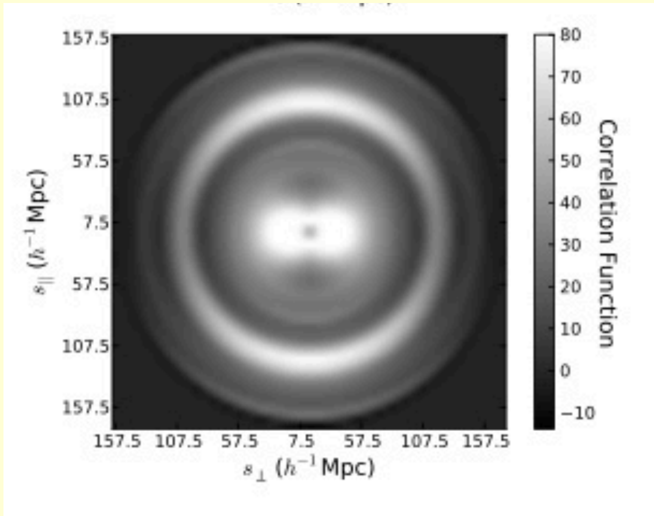

S. Alam et al., 2017, MNRAS,470, 2617A

1. A quick remider about the physics of BAO
2. Current results
3. Principle of the method

The plasma after primordial nucleosynthesis

- γ and **e**, **nuclei** (≡ionized baryons) in thermal equilibrium

  atom formation ↔ Compton scattering : as long as $\Gamma_{Compton}$>H(t)

- dark matter falling into gravitational wells increases primordial over-densities, making the photon-baryon plasma to oscillate into and out of the over-densities : 'acoustic oscillations' in primordial plasma

- end of equilibrium: T~0.26 eV (3,000K) $z \sim 1100 \equiv z_*$

  e & nuclei combine, $\sigma_{\gamma\text{-}b}$ drops, matter-radiation decouple after last-scattering

- At decoupling: oscillation pattern is frozen ⇒ imprint in CMB spectrum and matter spectrum (with a suppression factor Ω_b/Ω_m ~0.17)

Evolution of a single overdensity with time

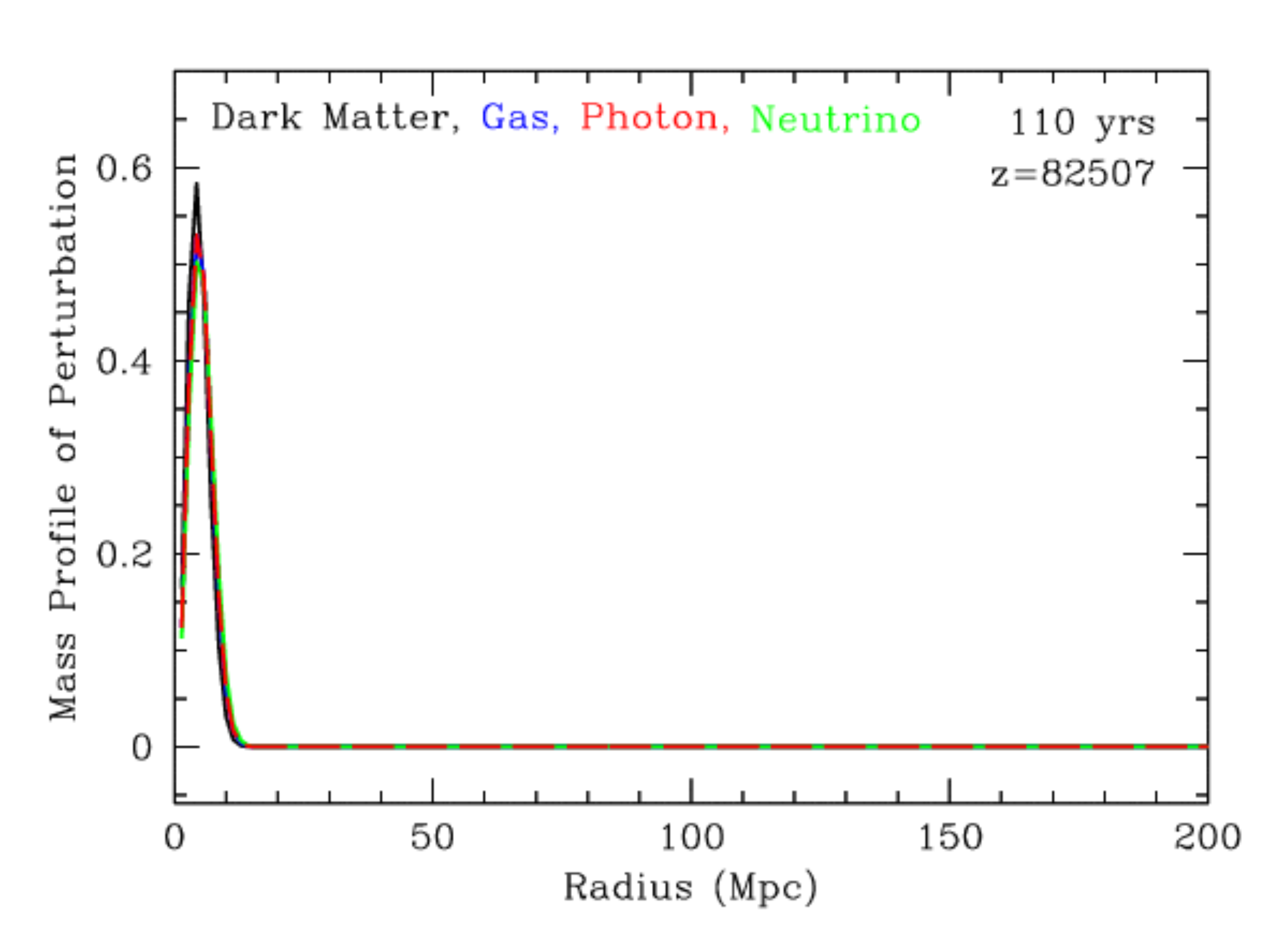

http://online.kitp.ucsb.edu/online/primocosmo-c13/eisenstein/vid/acoustic_anim.gif

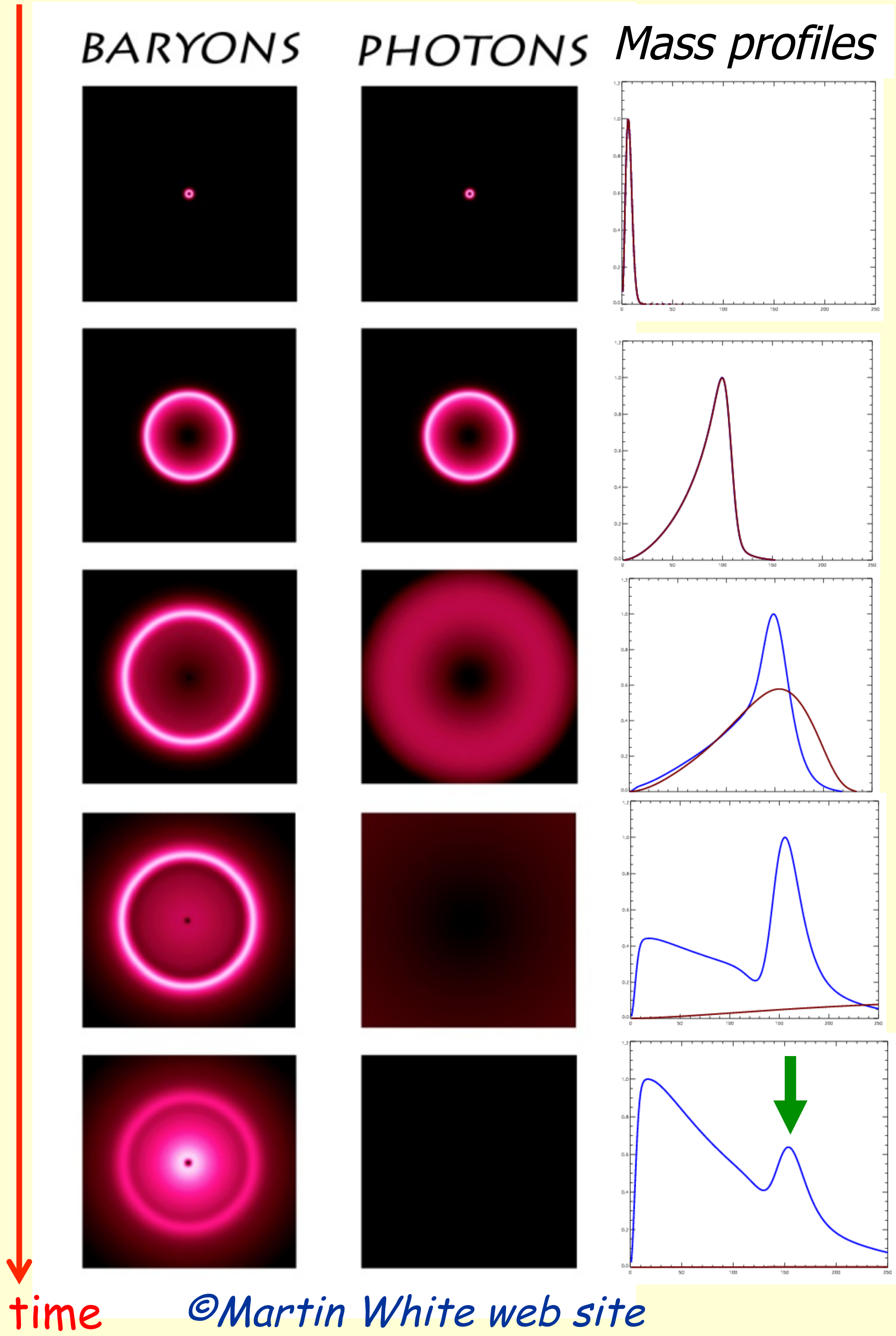

- one single overdensity in the plasma, moving outward
- γ and baryons move together, for 10^5 years
- decoupling: γ decouple from baryons and stream away, leaving the baryon peak stalled
- γ ~uniform, baryons remain overdense in a shell ~150Mpc in radius (comoving sound horizon)
- matter attracted by central DM pot. well -> residual shell at 150Mpc, observable today in the matter distribution

Results

BAO, 1st evidence, 2005

Two teams: SDSS and 2dFGRS

D.Eisenstein et al., 2005, ApJ, 633, 560

Galaxy correlation function

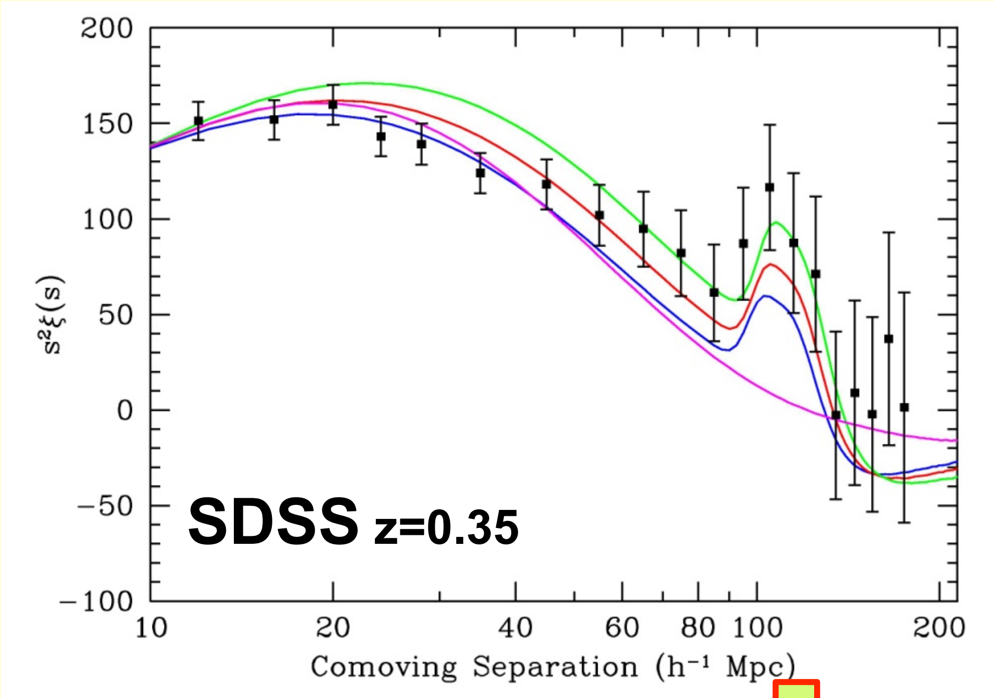

preferred comoving separation
~100h^{-1}Mpc≈150Mpc

(reminder: $h=H_0/100\sim0.7$)

Galaxy power spectrum

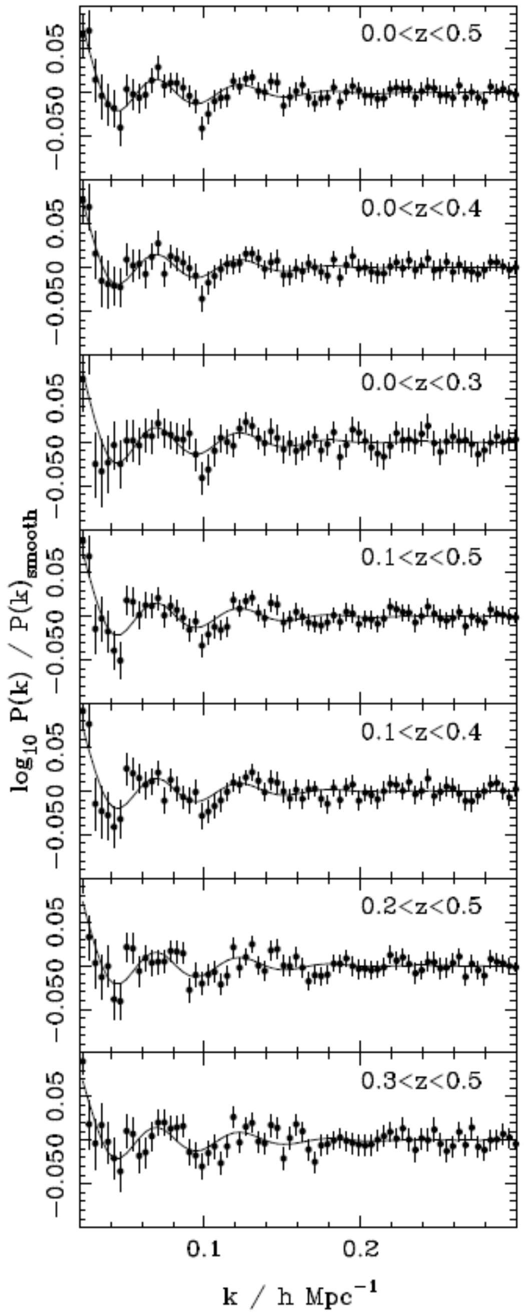

W.Percival et al., 2010, MNRAS, 401, 2148

SDSS-III/ BOSS *2017*

8σ detection of BAO peak in galaxy clustering
(9,329 deg^2, 1.2 10^6 galaxies)

S. Alam et al., 2017, MNRAS, 470, 2617A

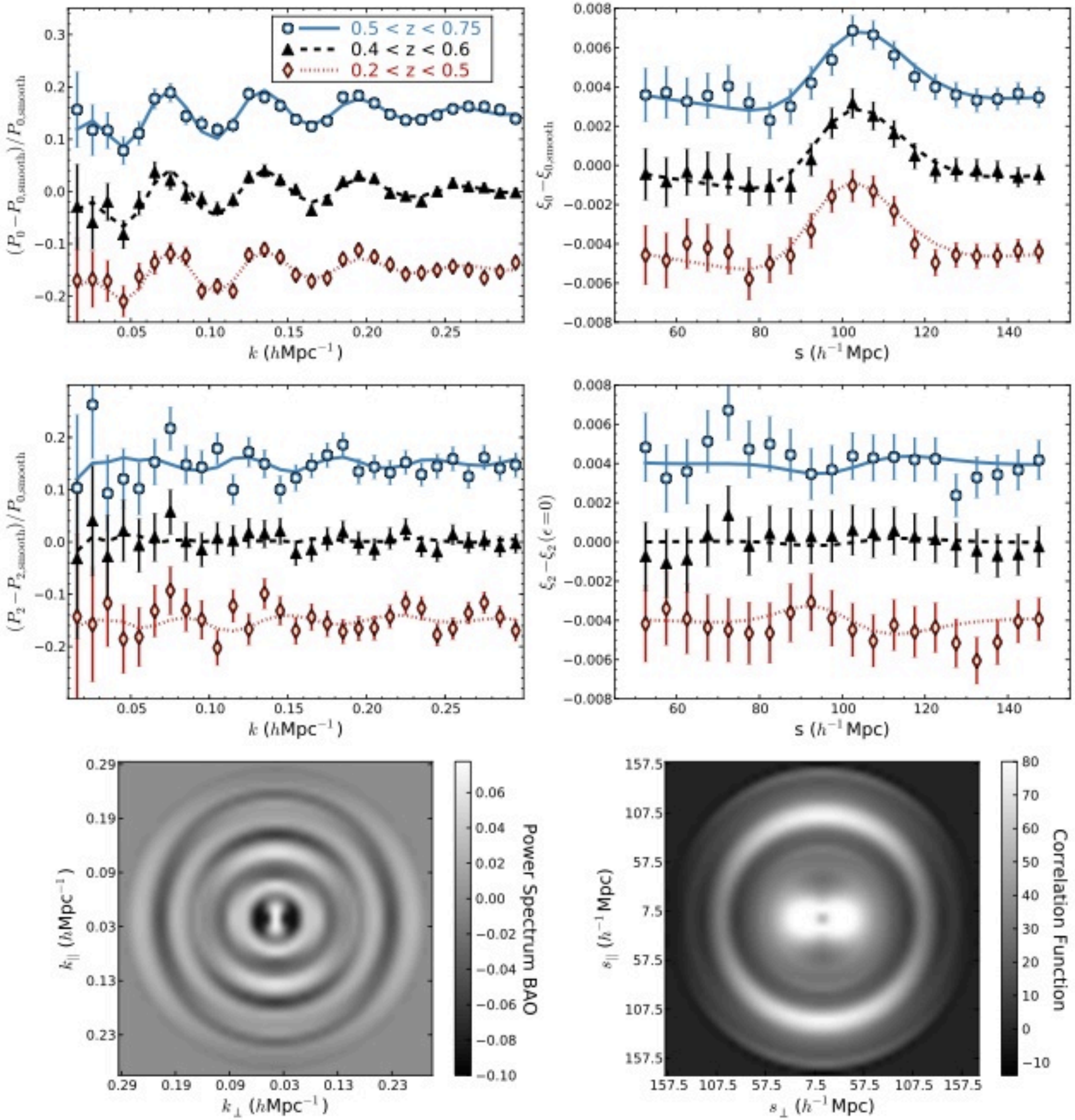

Beyond galaxies

- BAO signal also detected in clustering of intergalactic H clouds (via absorption lines in Lyα forest part of quasar spectra), quasars and in their cross-correlations.

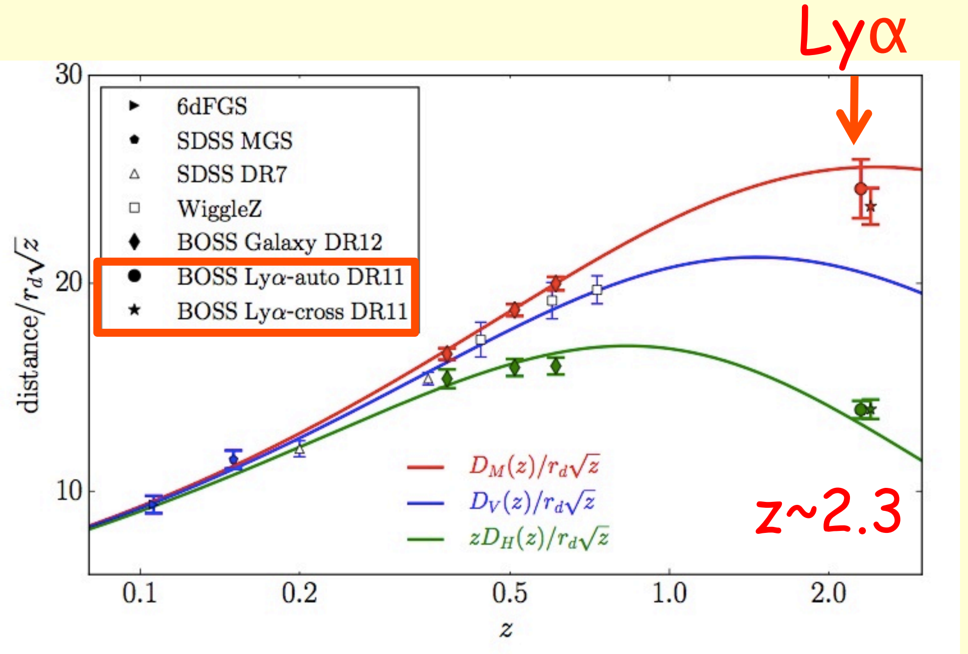

S. Alam et al., 2017, MNRAS,470, 2617A

SDSS-III/BOSS

Good consistency with Planck-alone Λ_{CDM} fit

Last update: SDSS-IV/eBOSS

V.de Sainte Agathe et al., A&A 629, A85 (2019)

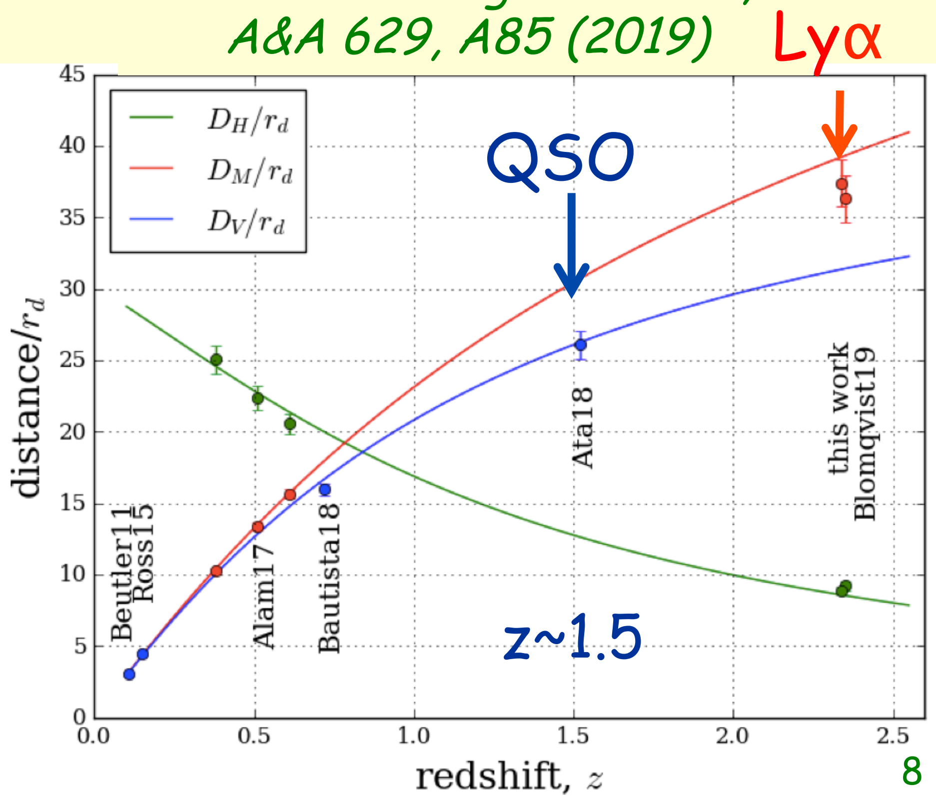

Method

BAO measurement

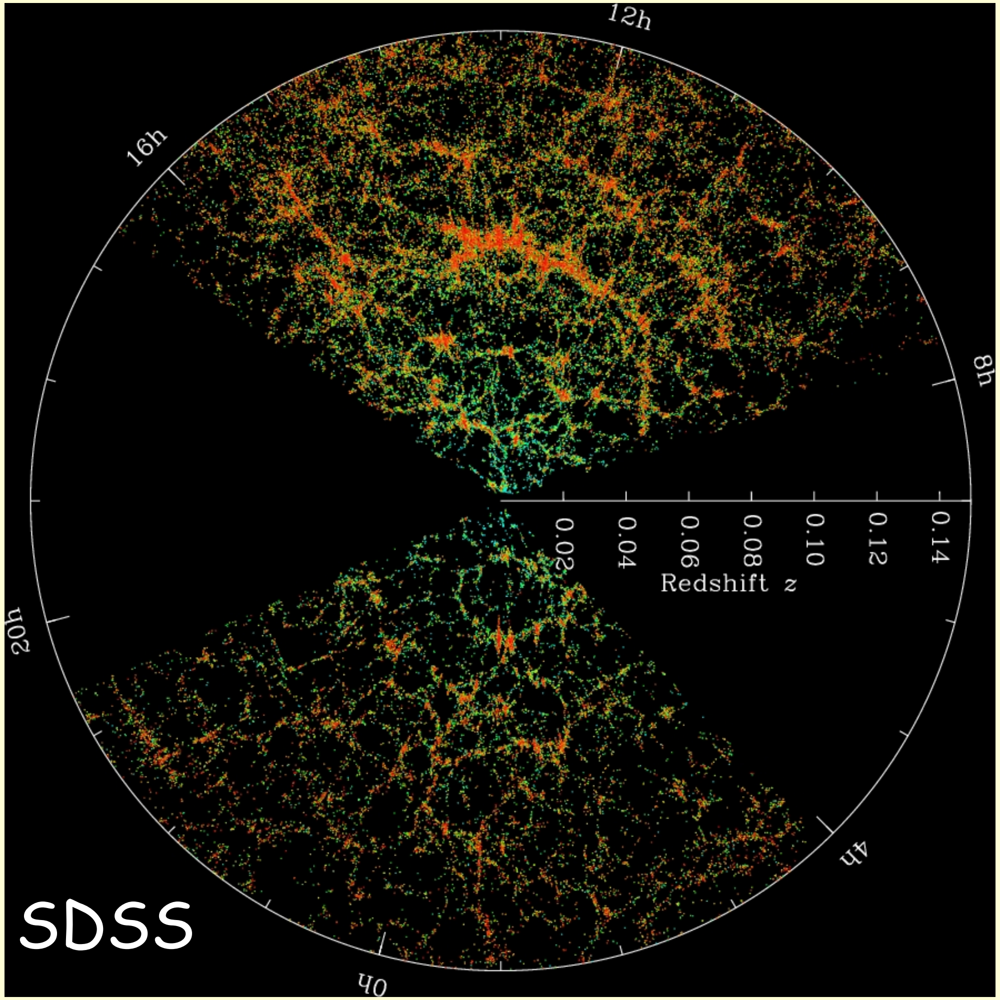

- data : ra,dec,z catalogue
- synthetic catalogue of random positions

  ⇒ density field:

$$\delta(\vec{r}) = \frac{\rho(\vec{r}) - \bar{\rho}}{\bar{\rho}}$$

- 2-point statistics : correlation function or power spectrum

  ⇒measurement of BAO signal (e.g. peak position in 2PCF)

BAO scale as a distance indicator

- 2-point statistics : correlation function or power spectrum

⇒measurement of BAO scale (e.g. peak position in 2PCF)

// l.o.s : $\Delta z(z) = r_d H(z)/c \equiv \frac{r_d}{D_H(z)}$ ⊥ l.o.s : $\Delta\theta(z) = \frac{r_d}{D_M(z)}$

with :

$$r_d = \int_{z_d}^{\infty} \frac{c_s(\tilde{z})d\tilde{z}}{H(\tilde{z})}$$

comoving sound horizon, $r_d(\Omega_i)$ ($c_s(\Omega_b/\Omega\gamma)$)
z_d = end of the Compton drag epoch $\lesssim z^*$

and e.g. in a flat ΛCDM Universe (and for z<<z*):

$$H(z)/H_0 = \sqrt{\Omega_m(1+z)^3 + \Omega_\Lambda} \qquad D_M(z) = (1+z)D_A(z) = \int_0^z \frac{c\,d\tilde{z}}{H(\tilde{z})}$$

D_M comoving distance, D_A angular diameter distance

- Anisotropic BAO:

// and ⊥ l.o.s measurements

⇒ $D_H(z)/r_d$ and $D_M(z)/r_d$

- Isotropic BAO (limited sample):

angle-averaged measure

⇒ $D_V(z) = \left[c z D_M^2(z)/H(z) \right]^{1/3}$

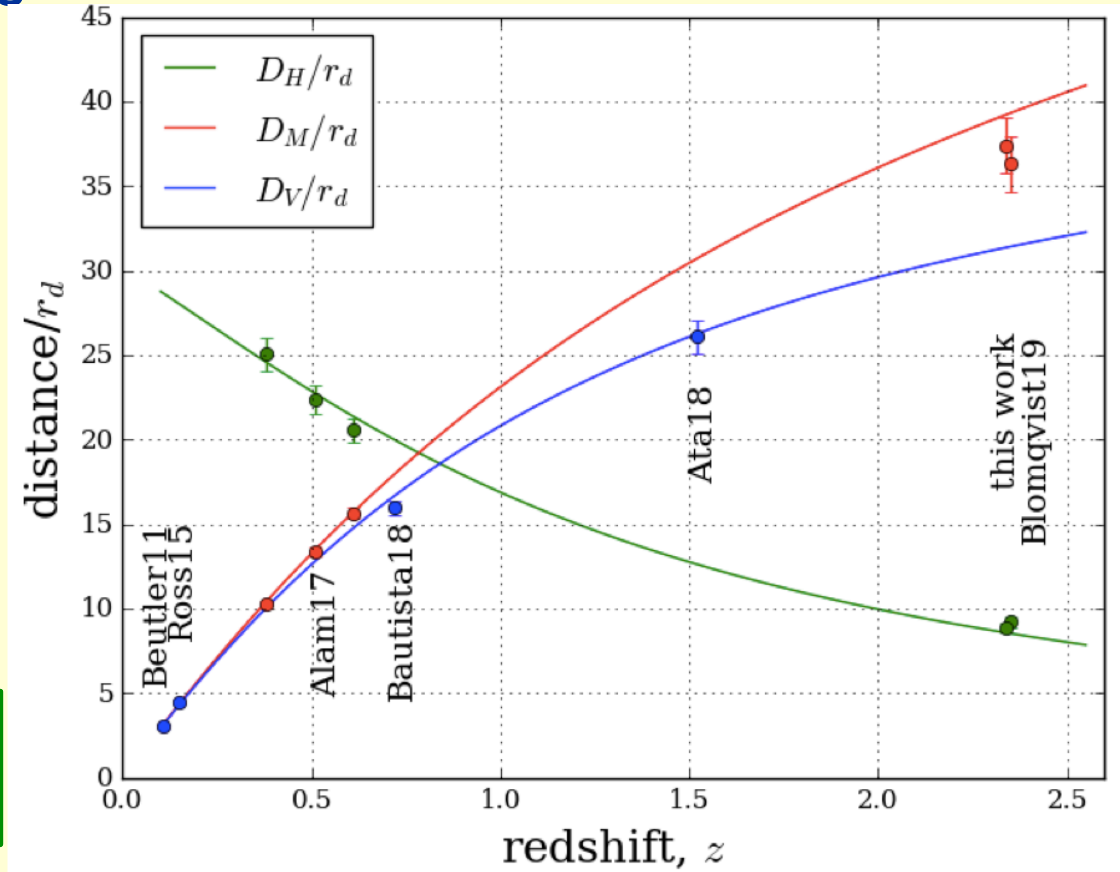

V.de Sainte Agathe et al., A&A 629, A85 (2019)

Tracers of matter

- Baryonic matter as tracer of total matter distribution, e.g.

$$\delta_g(\vec{k}) \approx b\delta_m(\vec{k})$$

b: tracer linear bias
(nuisance parameter)

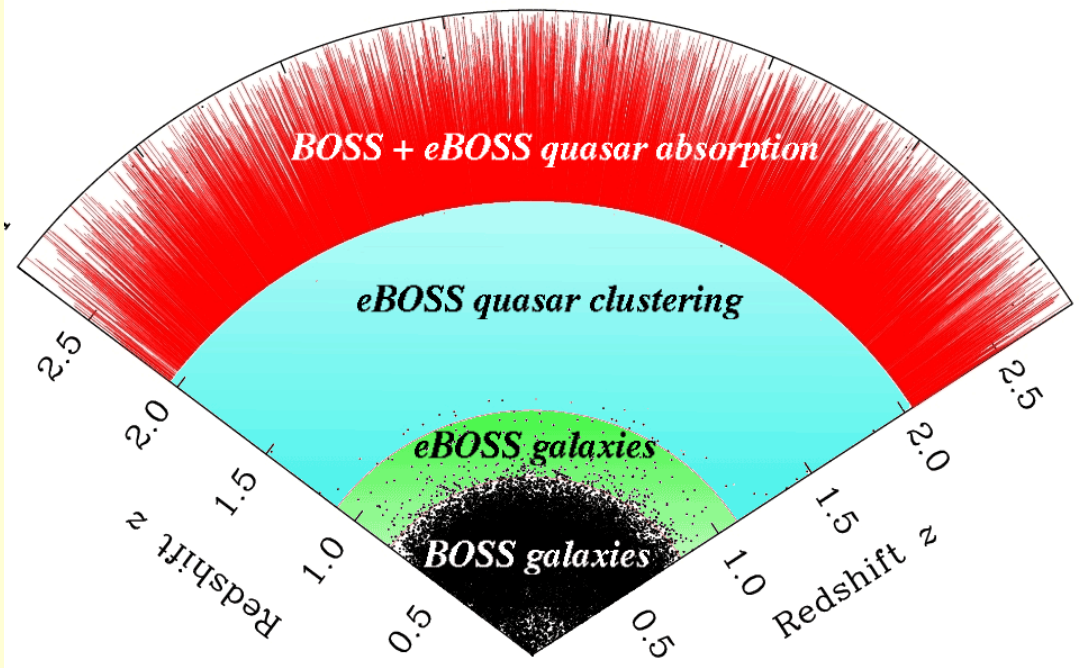

- Tracer choice per z bin: trade-off between luminosity and statistical uncertainty on P(k) or ξ(s) to be minimized
  - shot noise: $\sigma \propto P(k) \propto n$ n=tracer density

optimal density: $nP(k \approx 0.2hMpc^{-1}) \cong 1$ (dense survey, cosmic variance limited)

⇒highly biased tracers to be preferred since $P_g(k) \approx b^2 P_m(k)$

Robustness of the BAO scale measurement

- $\xi(s)$ = continuum + peak, observational systematics and continuum model have no impact on measured peak position, BAO scale → distances: linear physics

- non-linear effects from structure formation ⇒ peak enlarged, position (almost) unchanged (0.2-0.5% shift)

- enlargement of the BAO peak can be partially corrected (shift ≲ 0.1%) by reconstruction of the tracer displacement map from data ⇒ sharper peak, higher significance

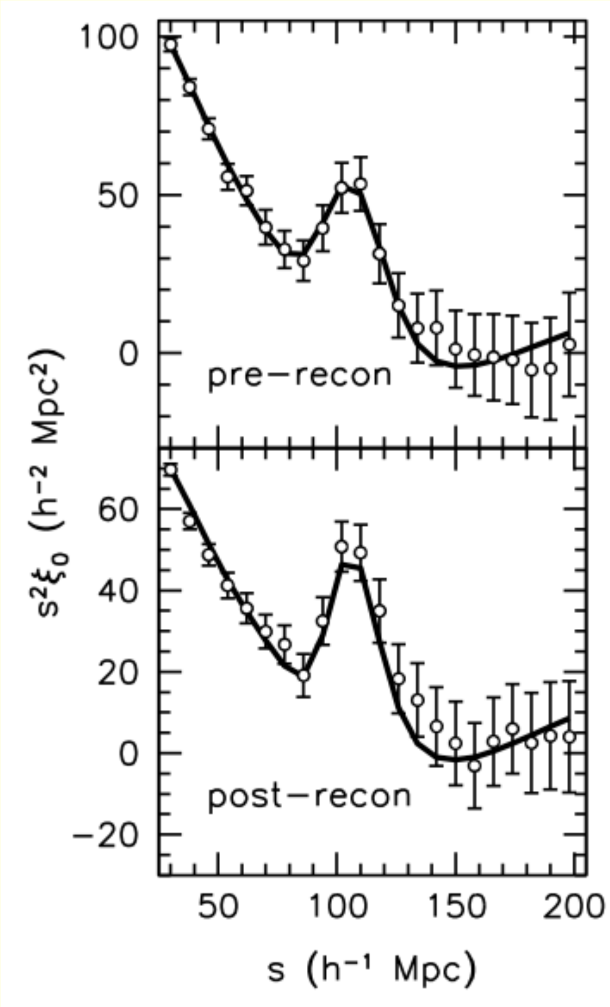

L. Anderson et al., 2014, MNRAS,441, 24A

BAO Summary

- BAO analysis:

– measures $D_M(z)$ and $c/H(z)$ relative to comoving sound horizon (r_d), well constrained by CMB data:

r_d = 147.09 ± 0.26 ***Mpc*** (Λ_{CDM} fit, Planck 2018)

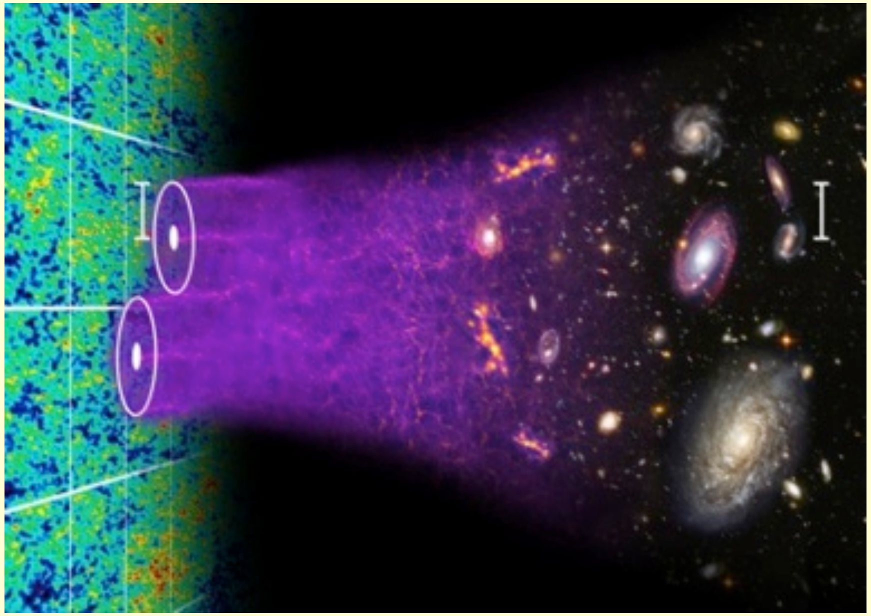

– peak position measurement robust against systematics;

– current uncertainties on distances : ≲5%, stat > syst

Beyond BAO (RSD)

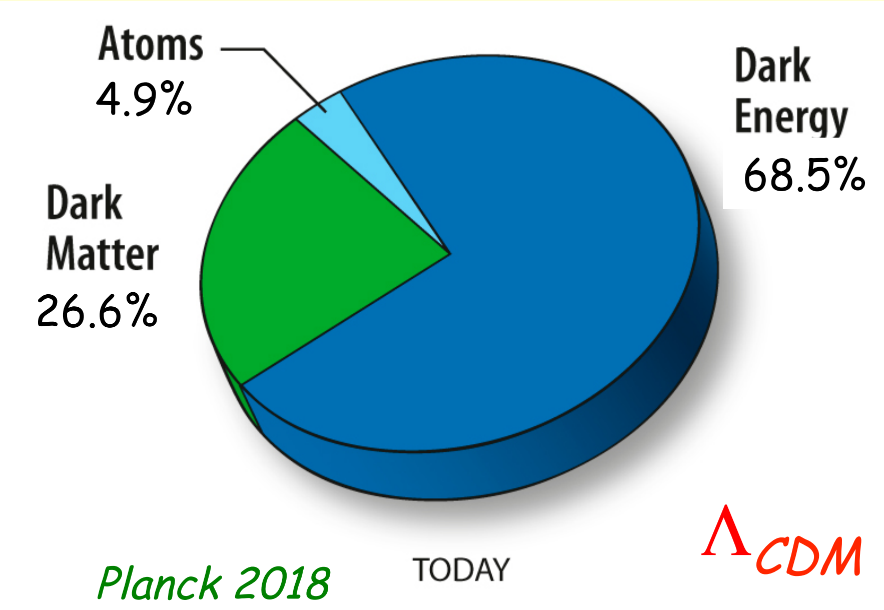

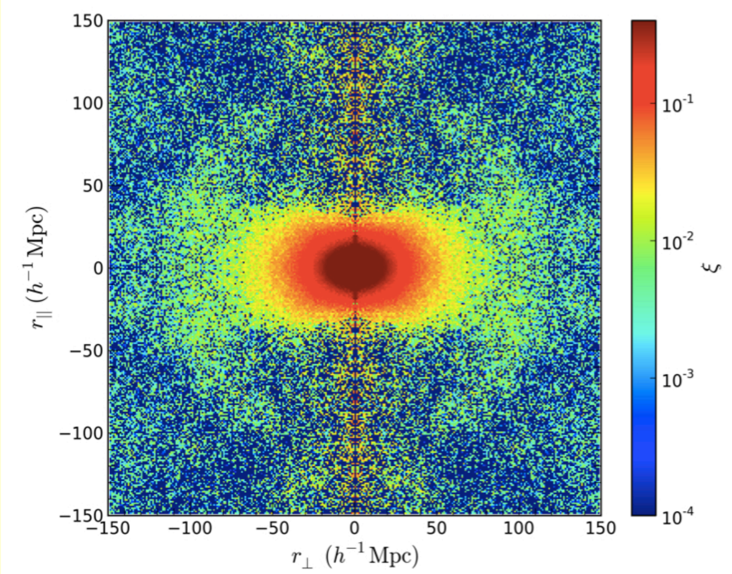

L.Samushia et al, 2014, MNRAS, 439, 3504.

1. Full shape analysis, principle of the method
2. Future prospects: DESI, LSST, WFIRST

From BAO …

Method

S. Alam et al., 2017, MNRAS,470, 2617A

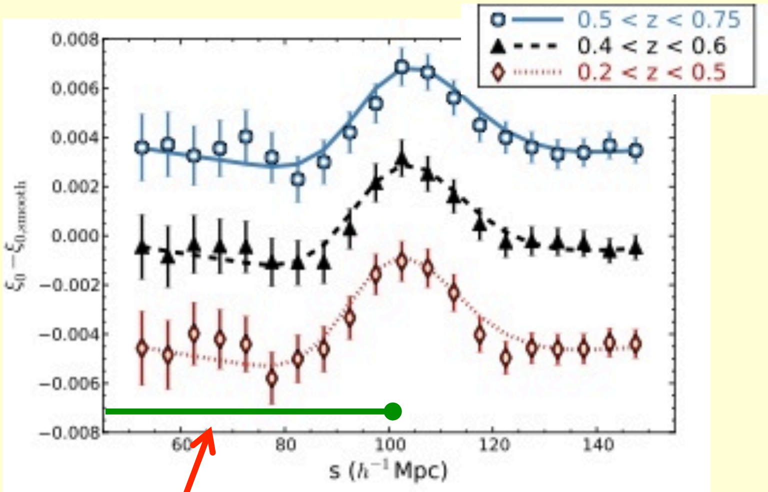

BAO scale

… to full shape analysis

S. Satpathy et al., 2017, MNRAS, 469, 1369S

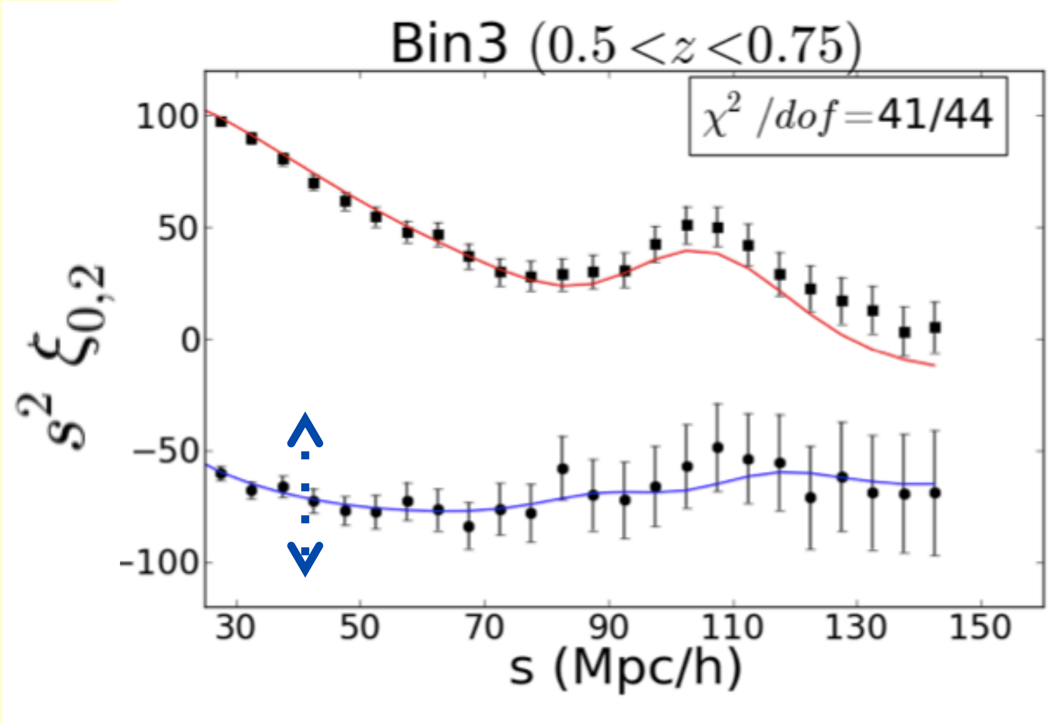

quadrupole amplitude = gravity strength

requires understanding of matter clustering on small scales (i.e. below BAO scale)

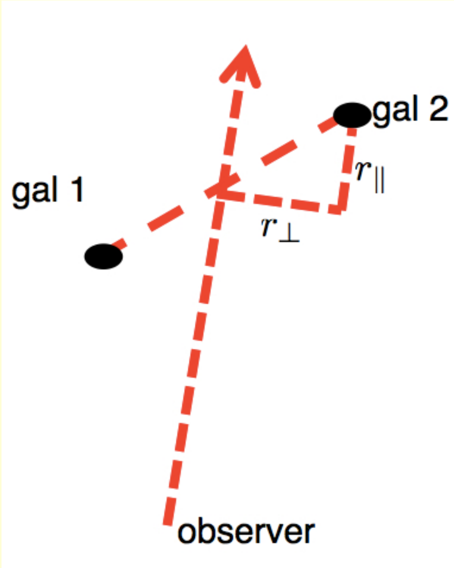

observed redshift: Hubble expansion + **peculiar velocity** due to gravity

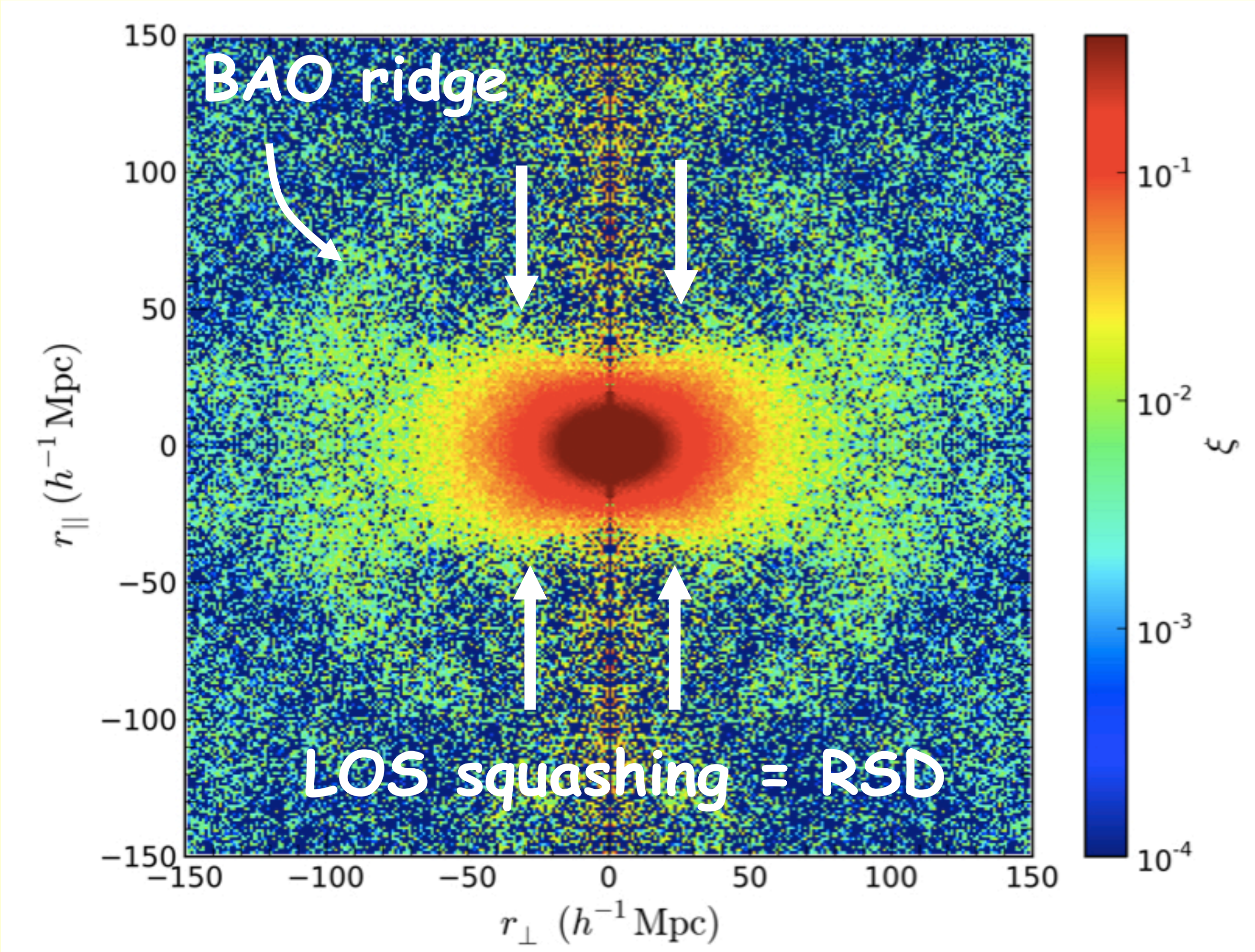

L.Samushia et al, 2014, MNRAS, 439, 3504.

Redshift Space Distortions : a way to test gravity -> full shape analysis and accurate modelling of correlation function required (tested on numerical simulations)

Recent results from full shape analyses :

- **Galaxies, z≈0.61,**
  Fourier space analysis, BOSS

F. Beutler et al., 2017, MNRAS,466, 2242

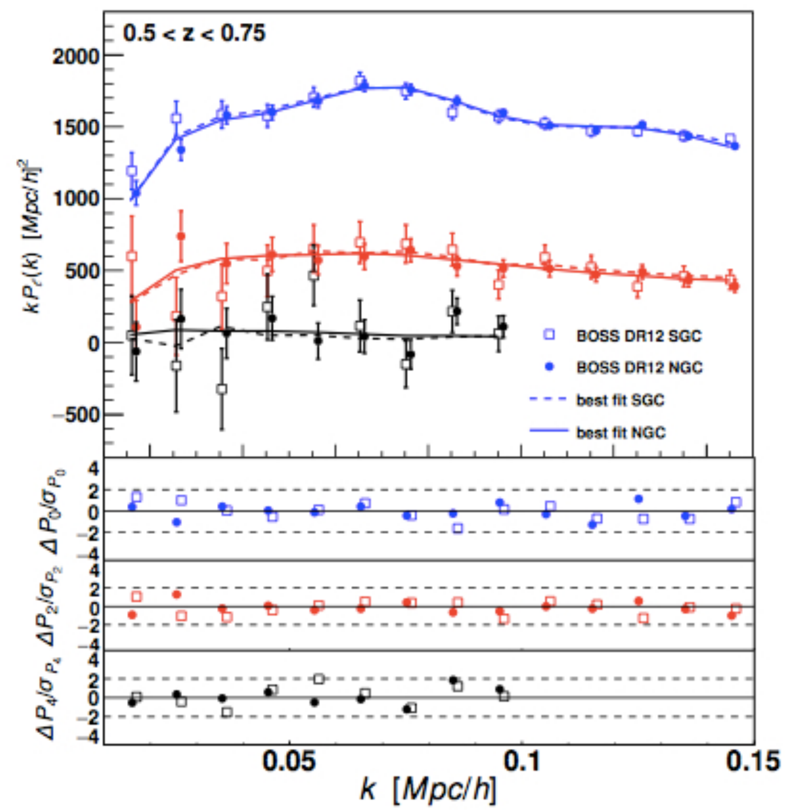

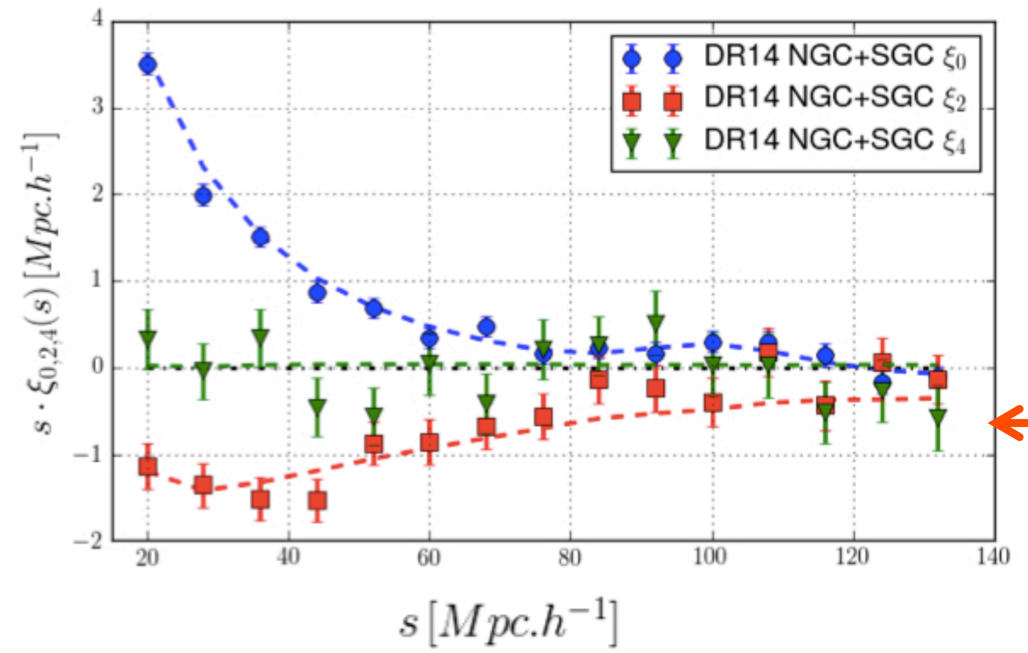

- **Quasars, z≈1.52,**
  Configur. space analysis, eBOSS

P. Zarrouk et al., 2018, MNRAS,477, 1639

- Full shape analysis:

⇒ $D_H(z)/r_d$ and $D_M(z)/r_d$

(used to constrain Alcock-Paczynski distortion)

and:

⇒ $f\sigma_8(z)$ with:

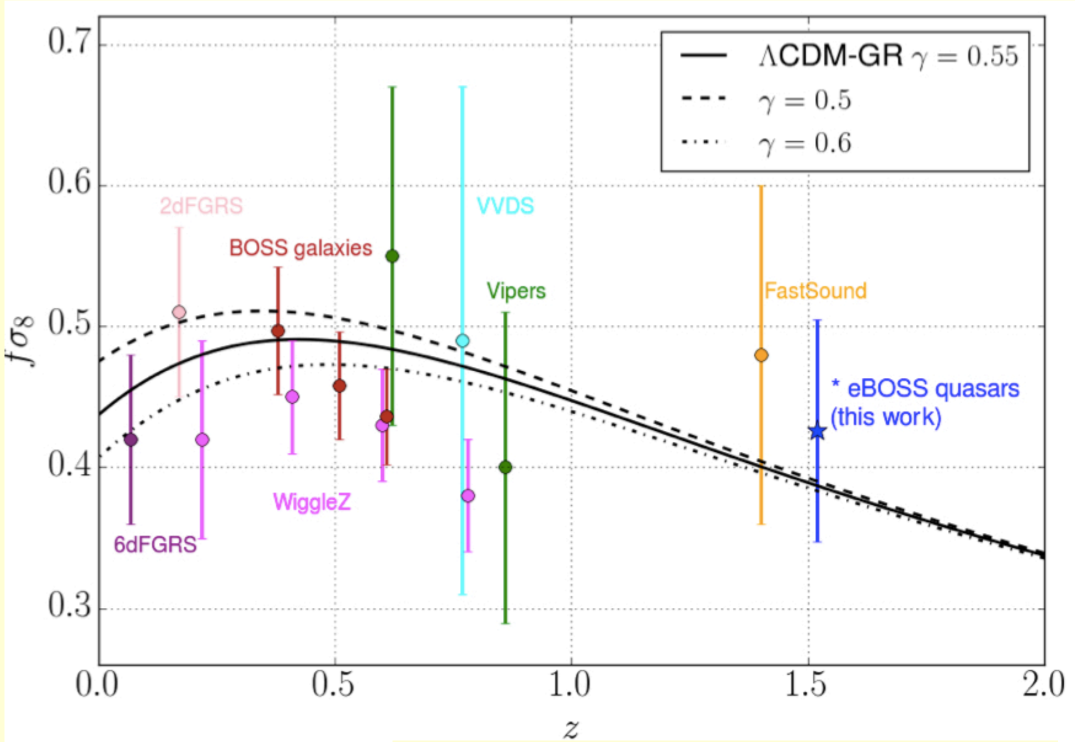

P. Zarrouk et al., 2018, MNRAS,477, 1639

$$f(z) \equiv \frac{d\ln D}{d\ln a}, \quad D(a) \equiv \frac{\delta_m(a)}{\delta_{m,i}} \equiv \frac{\delta\rho(a)\bar{\rho}_i}{\bar{\rho}(a)\delta\rho_i}$$

D(a) : linear growth function
f(z) : logarithmic growth rate of structures
$\sigma_8(z)$: matter power spectrum normalization (on 8 h^{-1}Mpc scale)

At present : few $f\sigma_8(z)$ measurements only, best accuracy ≈ 6-10%

RSD modelling

- Taruya, Nishimichi, Saito model (2010) used in BOSS/eBOSS:

$$P_g(k,\mu)=e^{-(fk\mu\sigma_v)^2}\left[P_{g,\delta\delta}(k)+2f\mu^2P_{g,\delta\theta}(k)+f^2\mu^4P_{\theta\theta}(k)+b^3A(k,\mu,f)+b^4B(k,\mu,f)\right]$$

Finger of God effect (incoherent velocities) $r_\sigma \ll 8h^{-1}$Mpc

Kaiser effect (large scale infall velocities) $r > 8h^{-1}$Mpc

TNS corrections

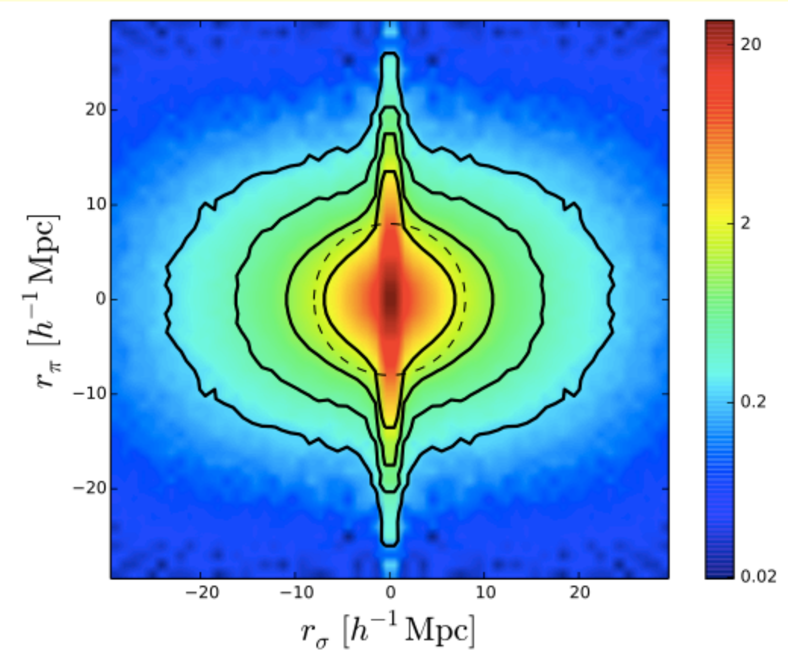

B. Reid et al., 2014, MNRAS,444..476R

- with:

$\mu \equiv \cos(\vec{k},\vec{u}_{los})$

$\sigma_v^2 \equiv \langle v_{los}^2 \rangle$

δ,θ ***density, velocity***

- and:

$P_{g,\delta\delta},P_{g,\delta\theta} \xleftrightarrow{\text{bias model}} P_{\delta\delta},P_{\delta\theta}$

$P_{\delta\delta},P_{\delta\theta},P_{\theta\theta},A,B$: *2-loop PT*

LSS Summary

- Full shape (= RSD) analysis :
  - provides BAO scales $D_M(z)$ and $c/H(z)$ relative to r_d and (linear) growth rate of structure $f\sigma_8(z)$
  - requires physical model of 2-point statistics in the non-linear regime (currently reliable up to $k\sim0.2hMpc^{-1}$)
  - impact of systematics (observ., model, analysis) larger % BAO
  - current uncertainties on growth rate : ~10% at best, stat > syst

- BAO and RSD analyses require:
  - wide surveys and large tracer densities
  - photometric target selection followed by spectroscopic survey
  - good control of systematics (photometric conditions, redshift failures, fiber collisions, analysis biases, 2-pt. stat. model ….) → mocks

Prospects

DESI

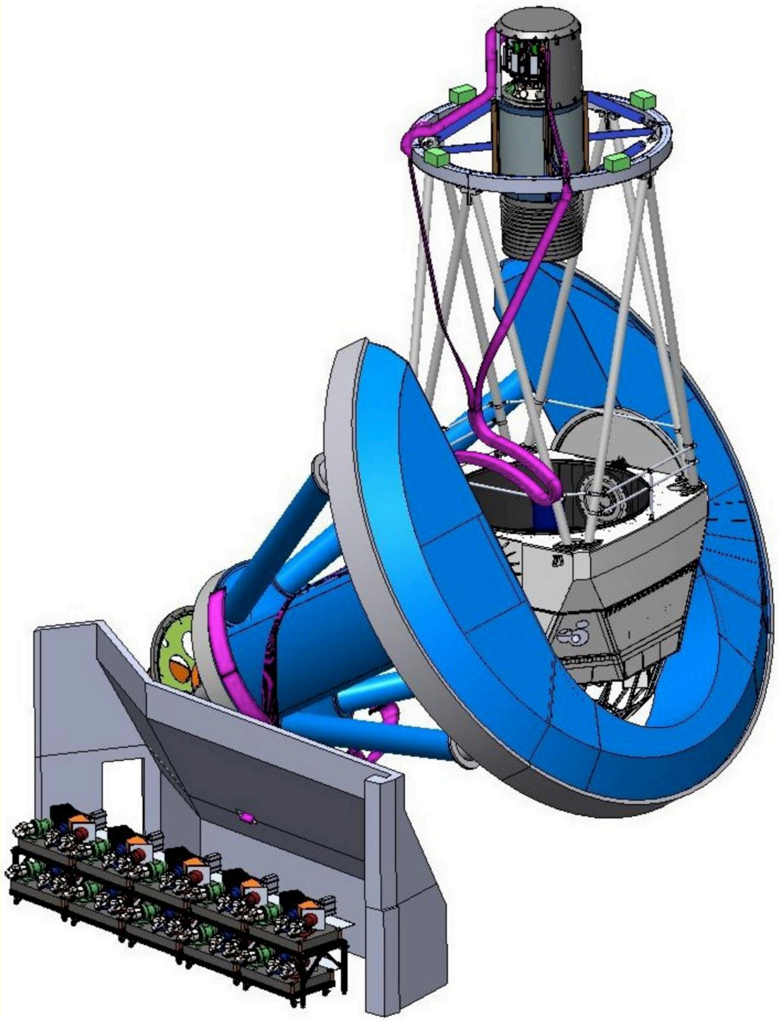

- 4 m mirror (Mayall telescope)
- 8 deg^2 FoV (new corrector)
- FP: 5,000 robotically positioned fibers
- 10 triple-arm spectrographs 360-980nm, $\lambda/\delta\lambda$=2000/4000
- Kitt Peak NO, Arizona
- 5 yrs from summer 2020
- 14,000 deg^2, 35 million redshifts

DESI: a wide spectroscopic survey dedicated to clustering measurements, BAO scales and growth rate

October, 22, first spectroscopic light in DESI !

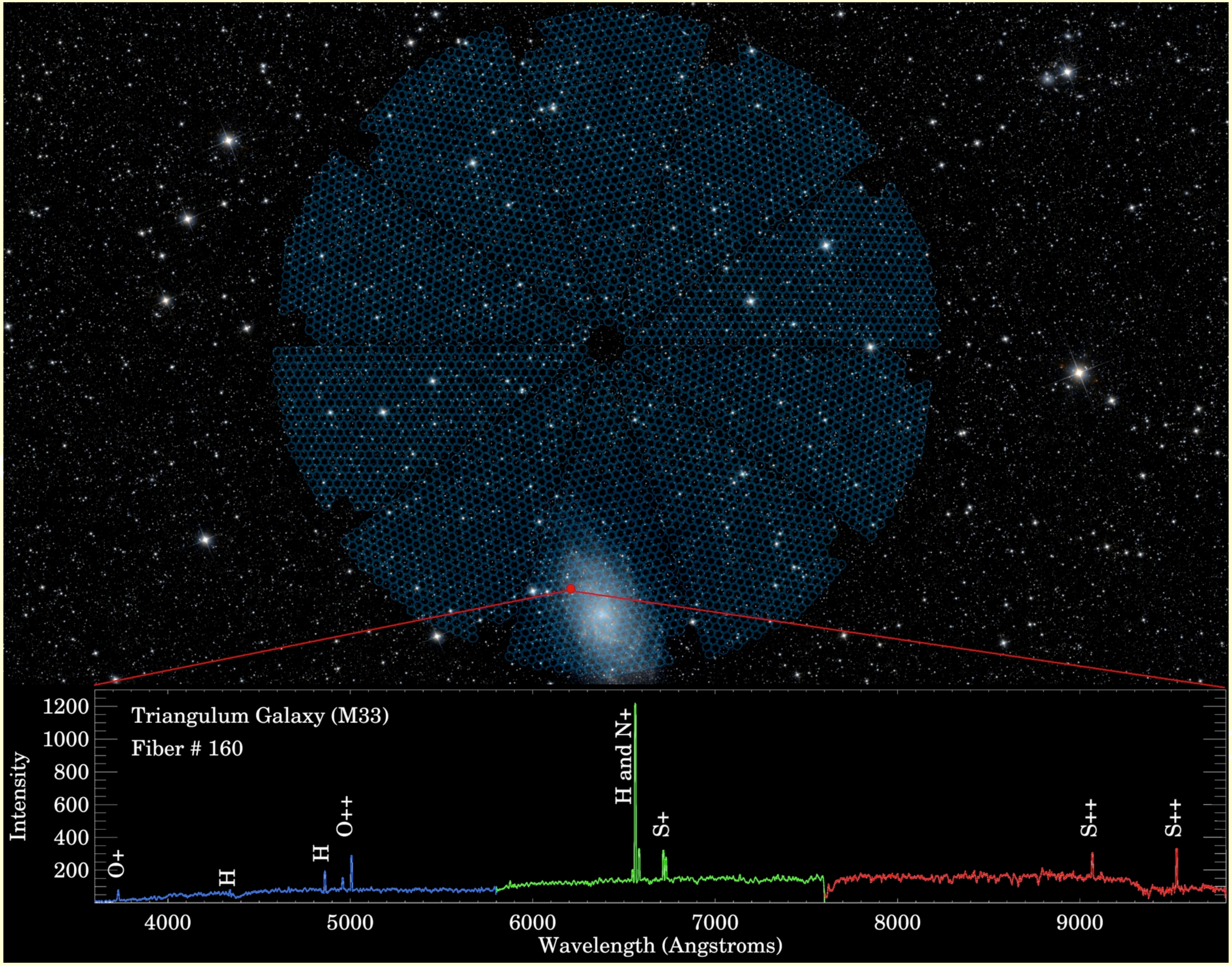

- DESI targets: BGs, LRGs, ELGs, QSO, Lyman-α forests
- From SDSS to DESI: data x 15

35 million galaxies, quasars / 14,000 sq.degrees / 0<z<4

BAO along the line of sight => H(z)

2019

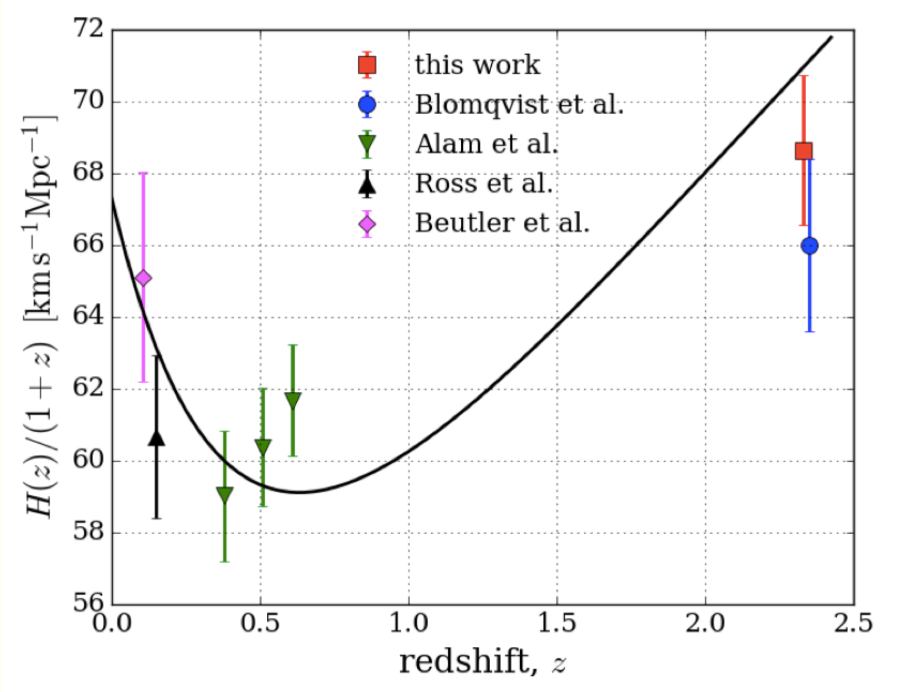

V.de Sainte Agathe et al., arXiv:1904.03400

29 z bins: δz=0.1 DESI

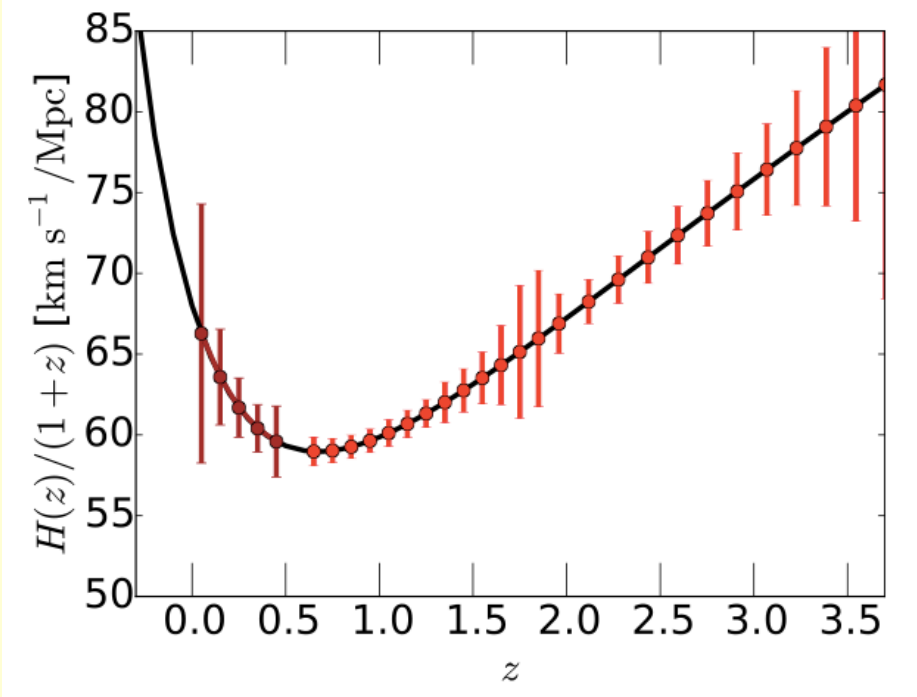

DESI prospects, arXiv:1611.00036

- DESI targets: BGs, LRGs, ELGs, QSO, Lyman-α forests
- From SDSS to DESI: data × 15

35 million galaxies, quasars / 14,000 sq.degrees / 0<z<4

Linear growth of structure rate

2018

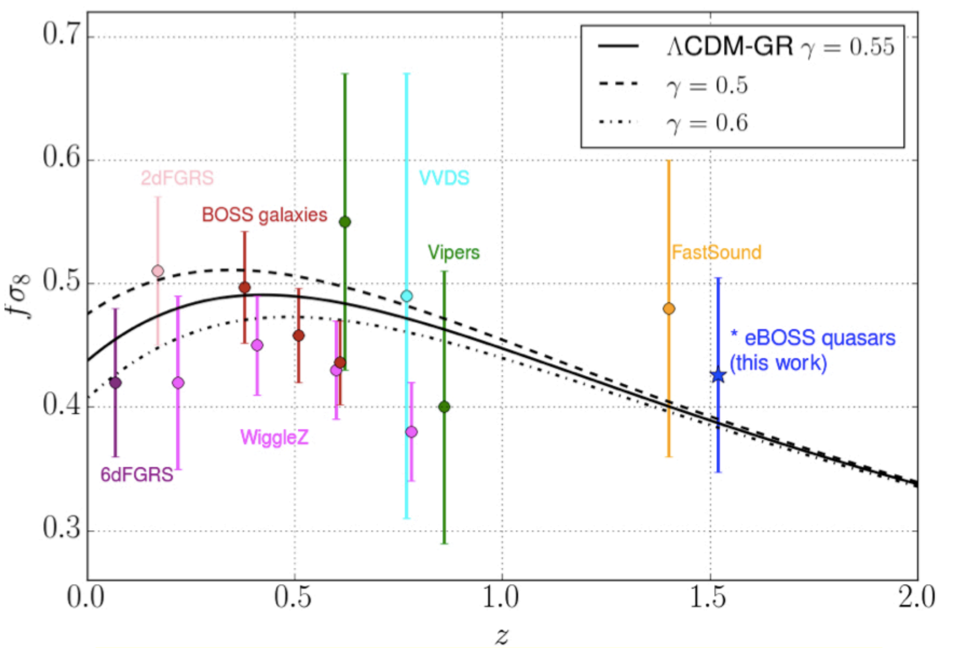

P. Zarrouk et al., 2018, MNRAS,477, 1639

18 z bins: δz=0.1 DESI

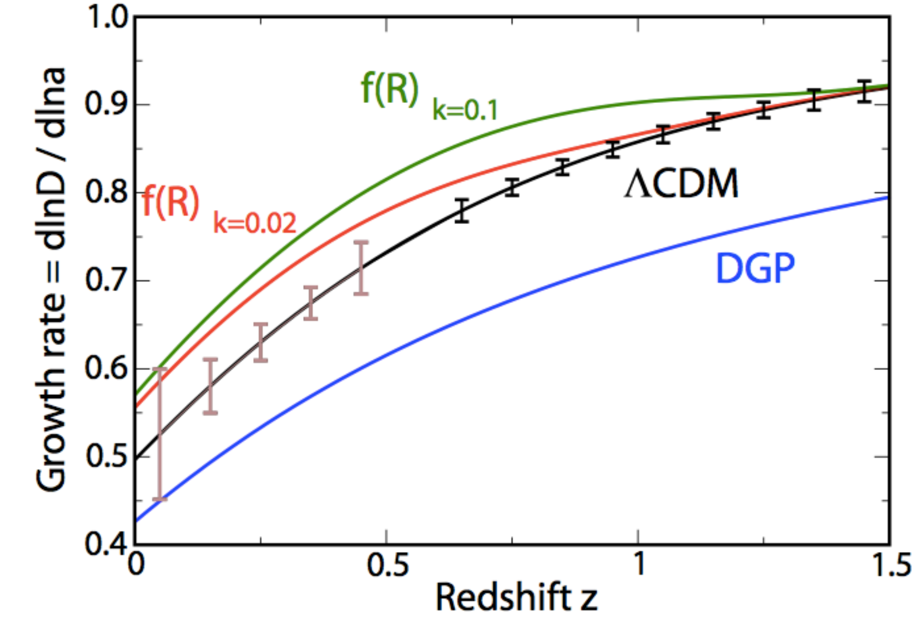

DESI prospects, arXiv:1611.00036

⇒ Forecast (BAO+RSD+Planck):

$\delta w_p = 0.01 \quad \delta w_a \approx 0.1$

Clustering with LSST

- LSST main survey : Wide-Fast-Deep survey (90%)
  18,000 deg^2, imaging 5σ point-source depth r_{AB}~ 27.5, 2 billion galaxies, photometric redshifts with $\sigma_z/(1+z)$~3%, bias<$3.10^{-3}(1+z)$

⇒tomographic clustering over 20 < ℓ < 15,000, in 10 (log) bins 0.14<z<3.6

(tomographic clustering ~ angular 2PCF)

z bins: $\delta\log(1+z)=0.1$

Z.Ivezic et al, arXiv:0805.2366v5 (May 2018)

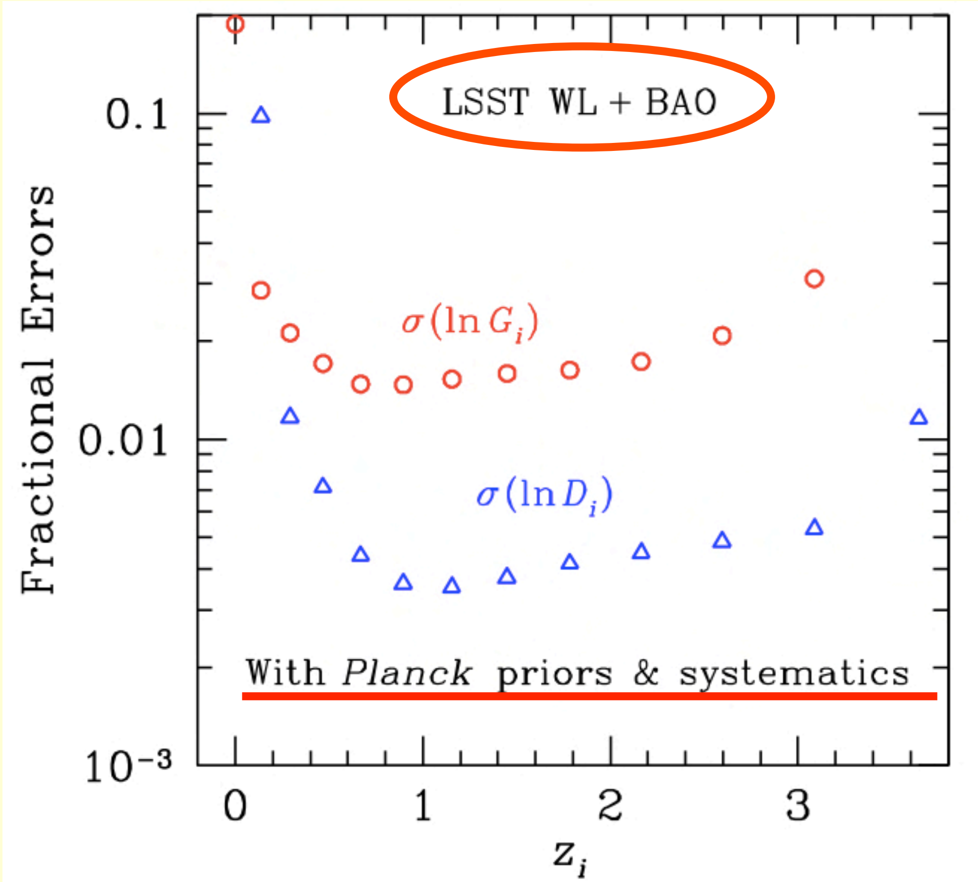

LSST forecast

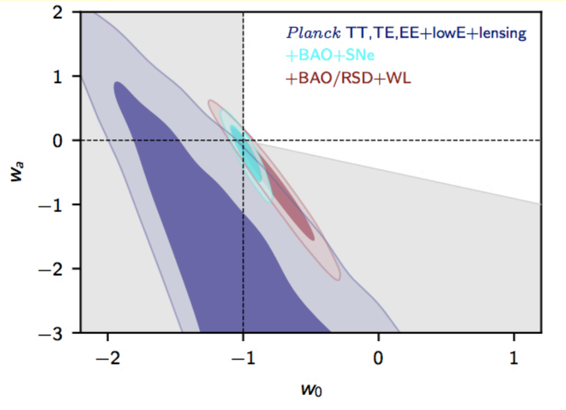

$\delta w = 0.032 = \delta w_p$

$\delta w_0 = 0.08 \quad \delta w_a \approx 0.3$

clustering & WL combined

dominant probe

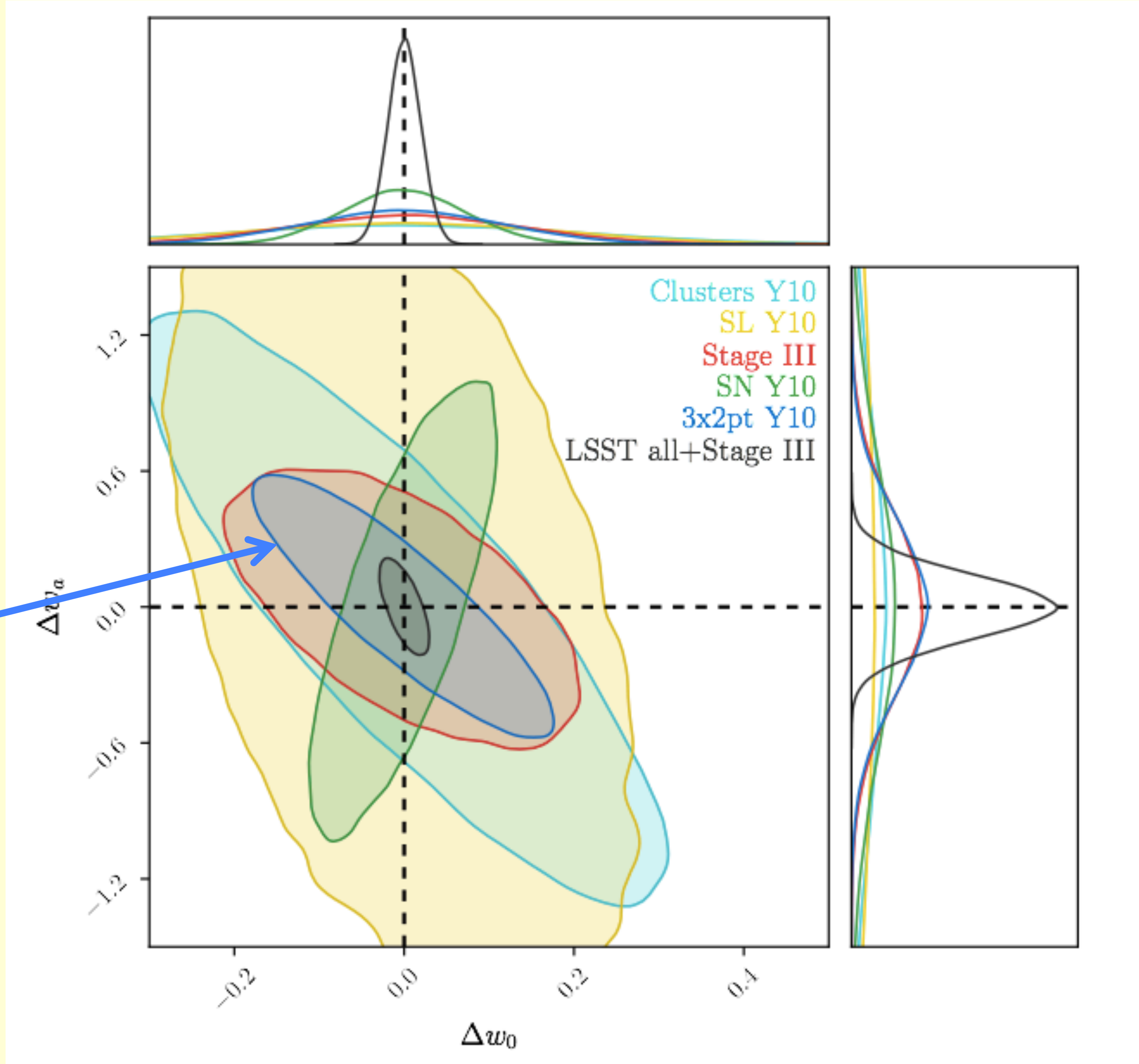

all probes:

$\delta w_0 \approx 0.025 \quad \delta w_a \approx 0.15$

LSST Dark Energy Science Collaboration, arXiv:1809.01669

Clustering with WFIRST

- WFIRST High Latitude spectroscopic Survey (2yrs over 5yrs):
  2,000 deg^2, imaging & grism spectroscopy, (5σ point source) depth Y,J,H,$F_{AB}\lesssim 27$, dense survey ($nP_{0.2}(z=1.5)=3.3$), 20 million redshifts , $0.5<z<2.9$ (Hα or [OIII] ELGs)

  Strong point: well-controlled systematics (high angular precision, photometric stability, low readout noise, coverage uniformity…)

z bins: $\delta z=0.5$

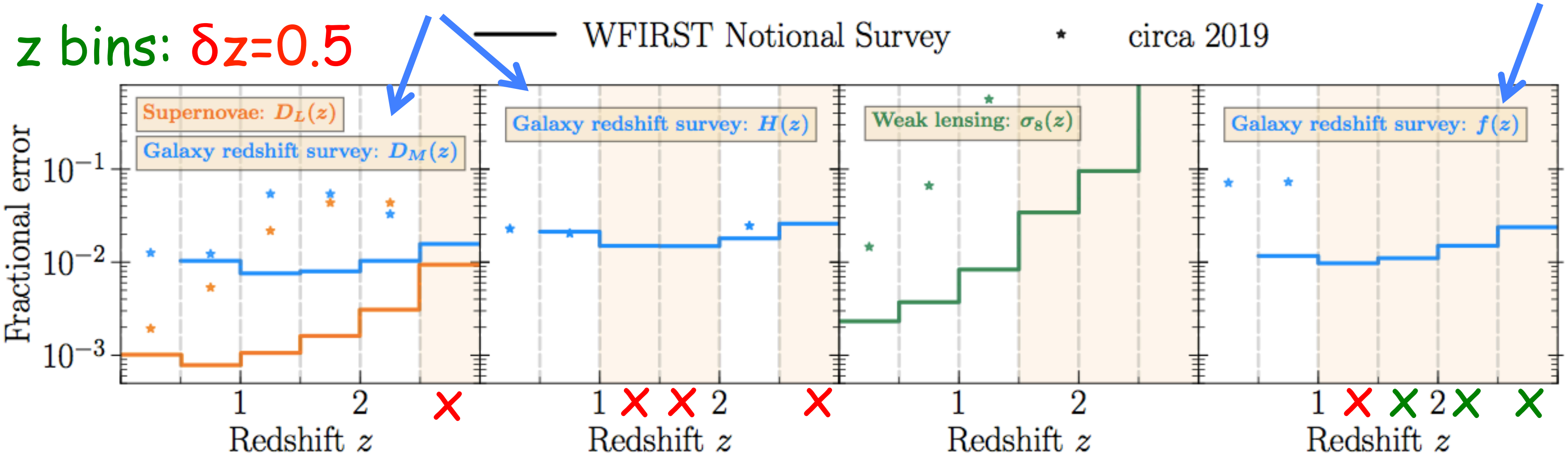

x = also probed by DESI/LSST with sub% / % accuracy

O. Doré et al, Astro2020 science white paper, arXiv:1904.011174

WFIRST forecast

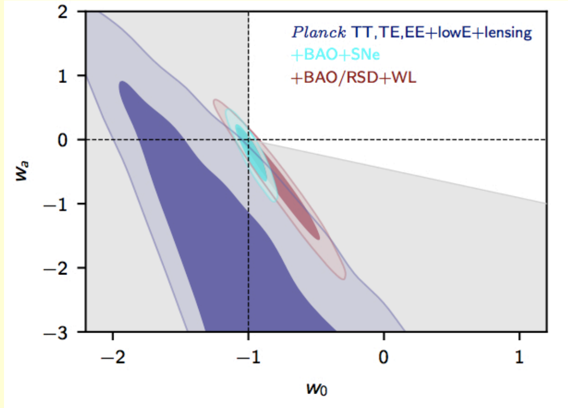

$\delta w = 0.032 = \delta w_p$

$\delta w_0 = 0.08 \;\; \delta w_a \approx 0.3$

BAO+RSD

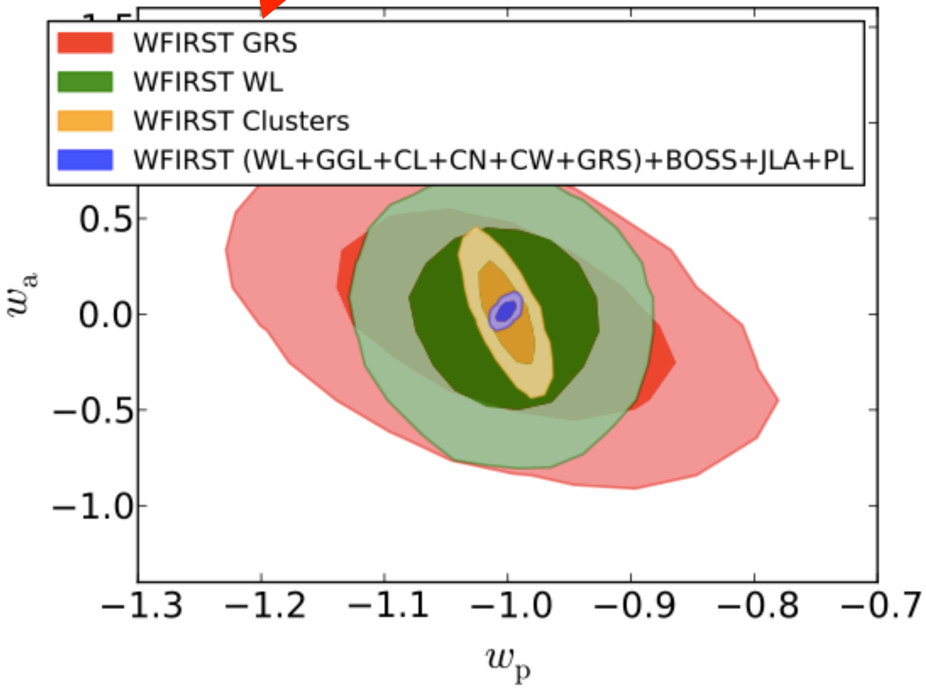

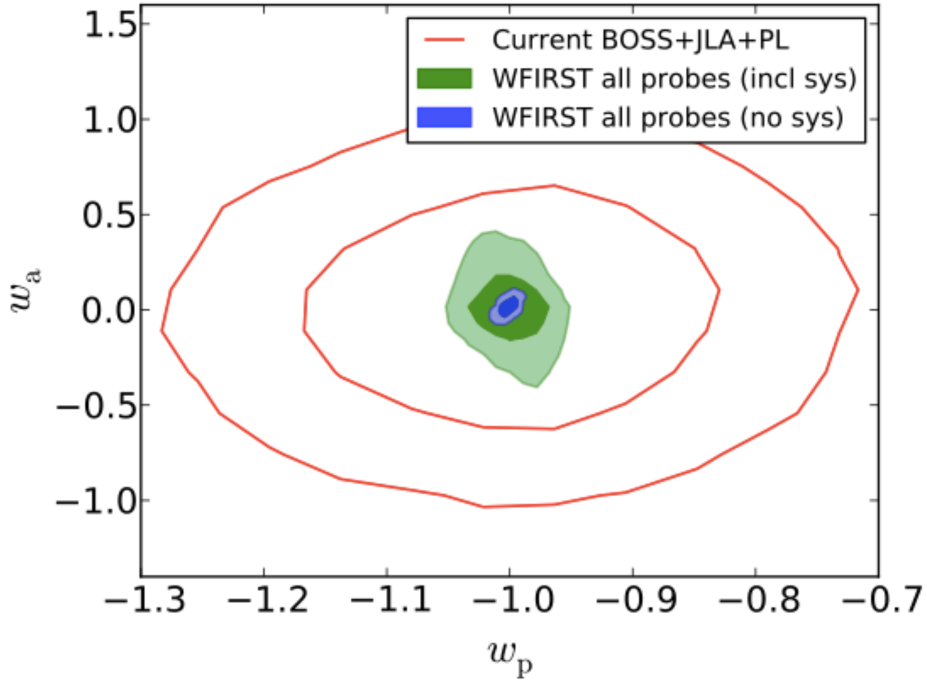

all probes: $\delta w_p \approx 0.025 \;\; \delta w_a \approx 0.13$

O. Doré et al, Cosmology with the WFIRST high latitude survey, arXiv:1804.03628

CONCLUSIONS

- BAO and RSD: probe sound horizon scale (relative to r_d) and growth rate of structures at various redshifts ; current uncertainties syst < stat

- RSD analyses require better control of non-linear regime in clustering modelling. Try other statistics than standard 2-point ones (count-in-cells, forward modelling).

- Prospects:
  - wide and dense surveys are coming : DESI, LSST, WFIRST…
  - BAO/RSD precise measurements at multiple redshifts soon available
  - promising: cross-correlations between tracers (voids x Galaxies, ELGs x LRGs …), cross-correlations RSD x WL (3x2pt) → see L3
  - complementarity between surveys: DESI & WFIRST/LSST at $z > 2$

Back up slides

Tracers of matter

	LRG	ELG	LAE	QSO	Lya	21 cm
bias	≈ 2	≈ 1	unknown	≈ 3	≈ 0.2	unknown
nP	dense	dense	dense	sparse	sparse	dense
z range	< 0.8	< 2	$2 - 3.5$	$1 - 2$	$2 - 3.5$	< 3

- LRG: Luminous Red Galaxies
- ELG: Emission-Line Galaxies
- LAE: Lyman-a Emitters
- QSO: quasars
- Lyman-a forest: intergalactic hydrogen clouds
- 21cm: hydrogen 21 cm emission line (radio detection)

Reconstruction: principle of the method

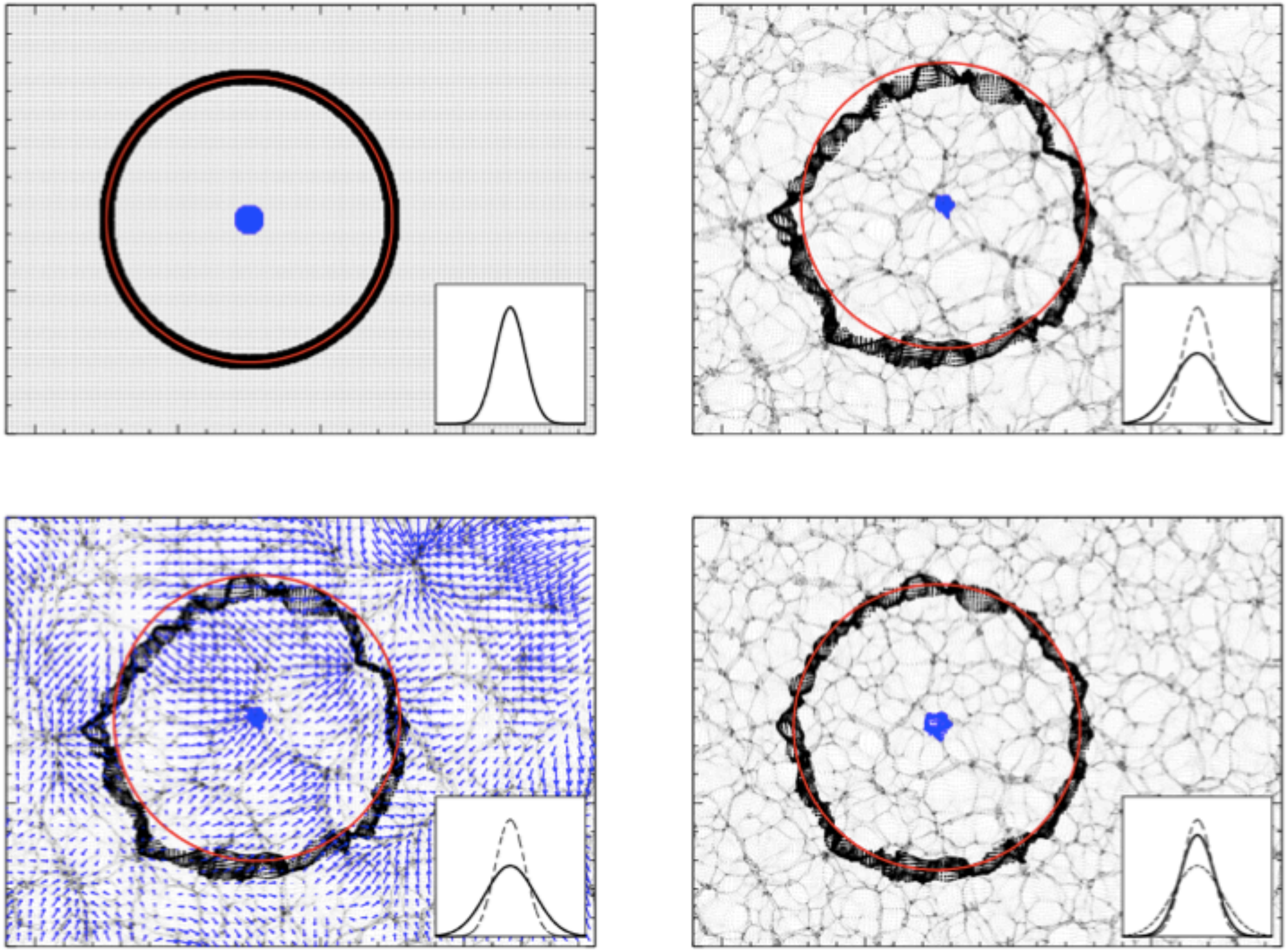

N. Padmanabhan et al., 2012, MNRAS,427, 2132P

Reconstruction

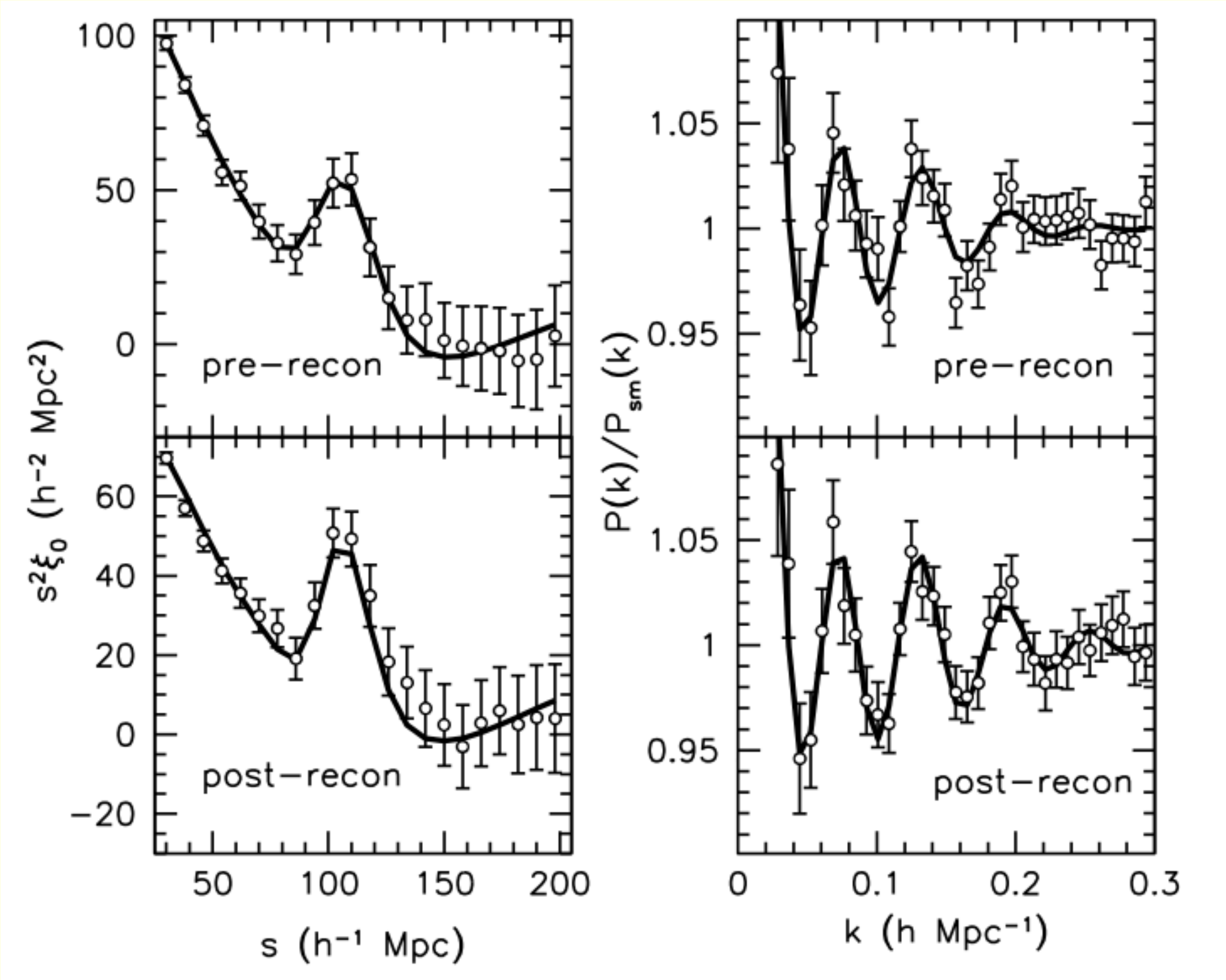

L. Anderson et al., 2014, MNRAS,441, 24A

Cosmological parameters and 2PCF

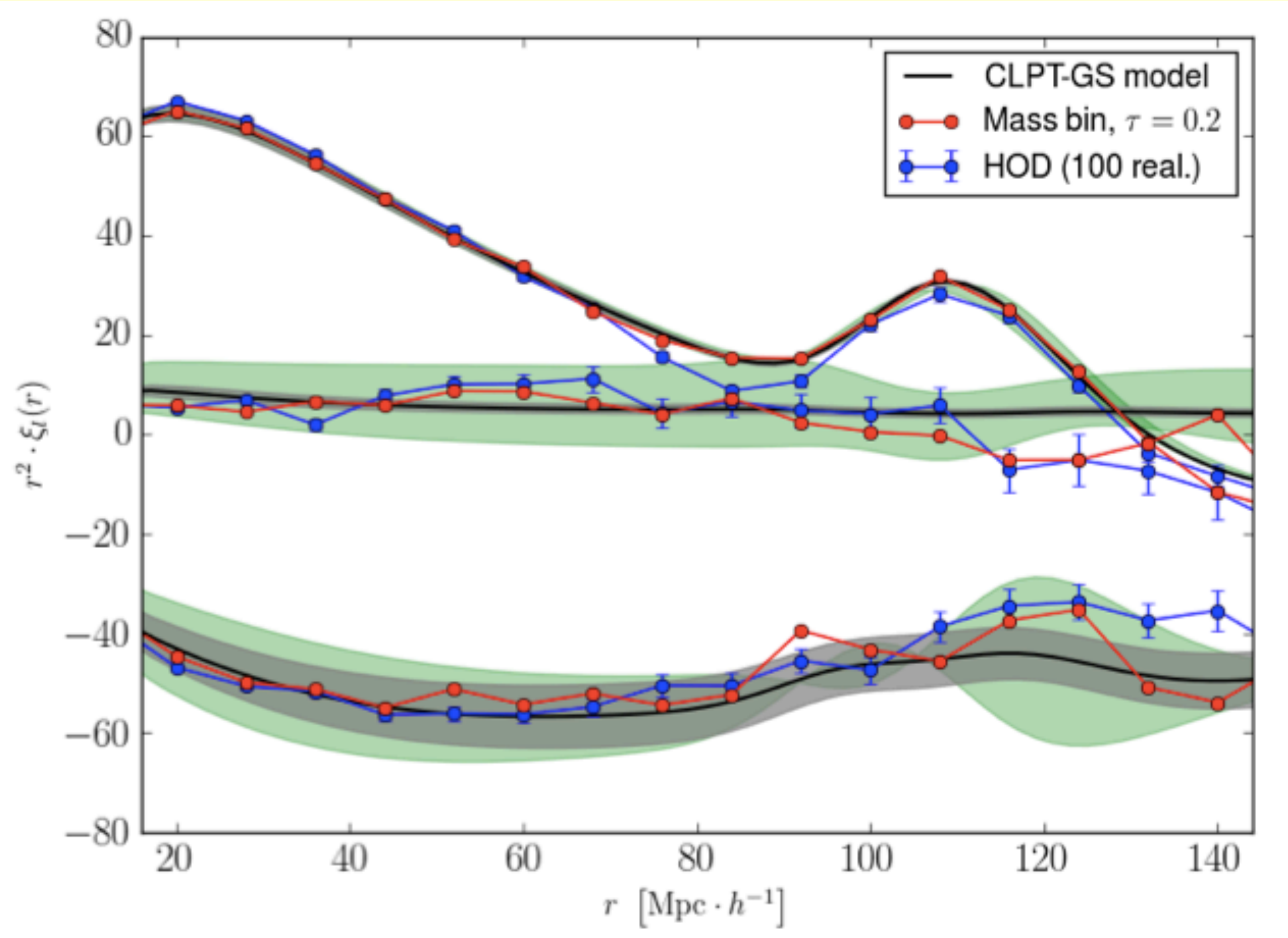

green: ± 10% on BAO scales

grey: ± 10% on growth rate

P. Zarrouk et al., 2018, MNRAS,477, 1639

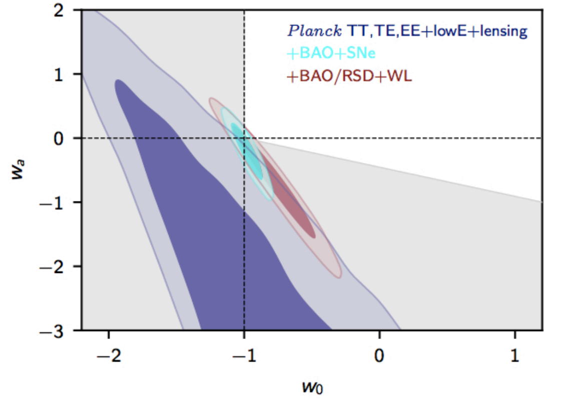

$w_0 = -0.96 \pm 0.08$

$w_a = -0.28^{+0.31}_{-0.27}$

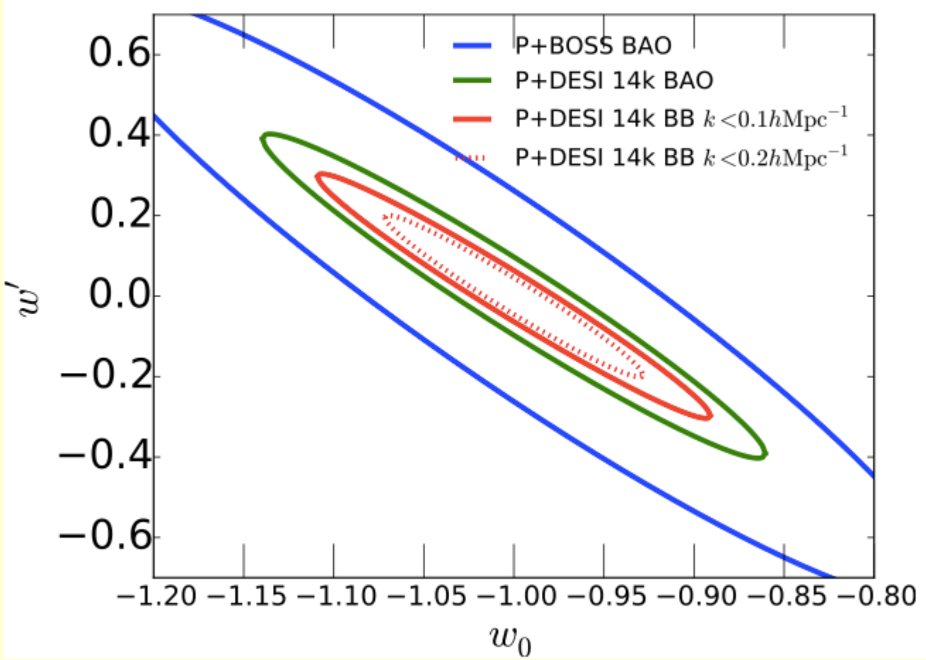

$w(z) = w_p + w'(a_p - a)$

Surveys	FoM	a_p	σ_{w_p}	σ_{Ω_k}
BOSS BAO	37	0.65	0.055	0.0026
DESI 14k galaxy BAO	133	0.69	0.023	0.0013
DESI 14k galaxy and Ly-α forest BAO	169	0.71	0.022	0.0011
DESI 14k BAO + gal. broadband to $k < 0.1\ h\ \mathrm{Mpc}^{-1}$	332	0.74	0.015	0.0009
DESI 14k BAO + gal. broadband to $k < 0.2\ h\ \mathrm{Mpc}^{-1}$	704	0.73	0.011	0.0007
DESI 9k galaxy BAO	95	0.69	0.027	0.0015
DESI 9k galaxy and Ly-α forest BAO	121	0.71	0.026	0.0012
DESI 9k BAO + gal. broadband to $k < 0.1\ h\ \mathrm{Mpc}^{-1}$	229	0.73	0.018	0.0011
DESI 9k BAO + gal. broadband to $k < 0.2\ h\ \mathrm{Mpc}^{-1}$	502	0.73	0.013	0.0009

DESI prospects, arXiv:1611.00036

The Mayall telescope at Kitt Peak observatory

DESI corrector

summer 2018

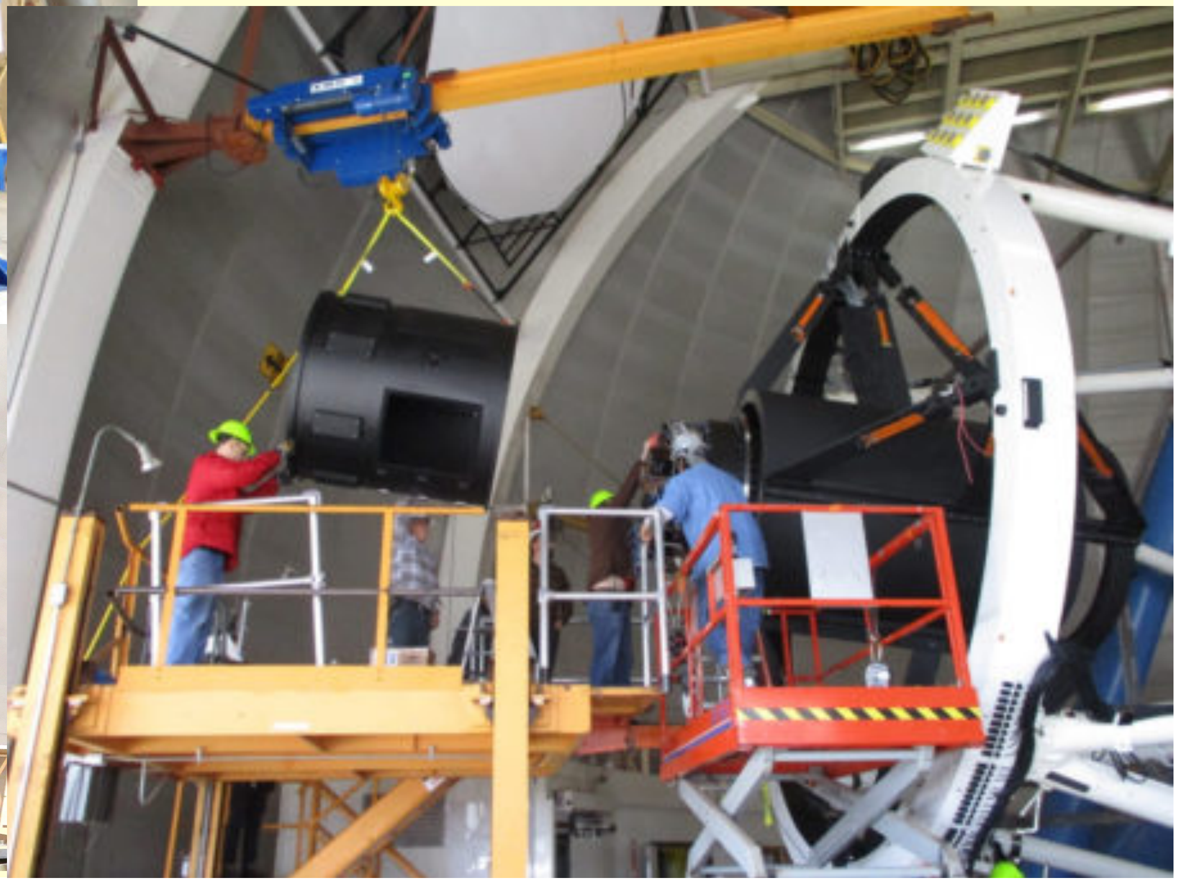

+ commissioning instrument

spring 2019

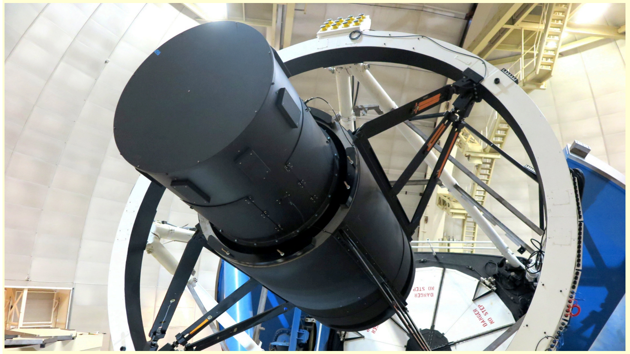

DESI corrector commissioning

April 2019

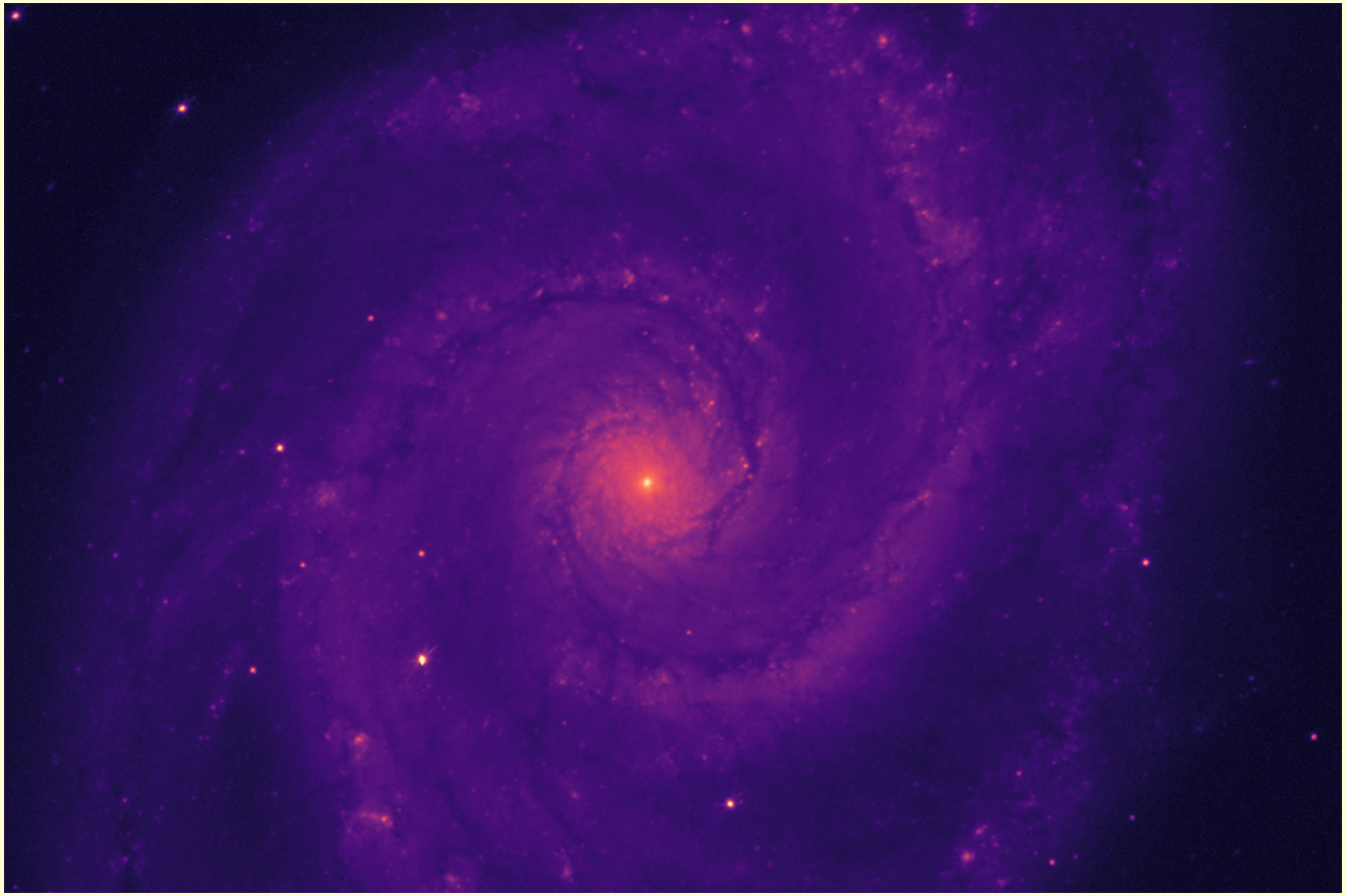

the Whirlpool galaxy seen through the DESI corrector lenses

February 2019

DESI spectrographs

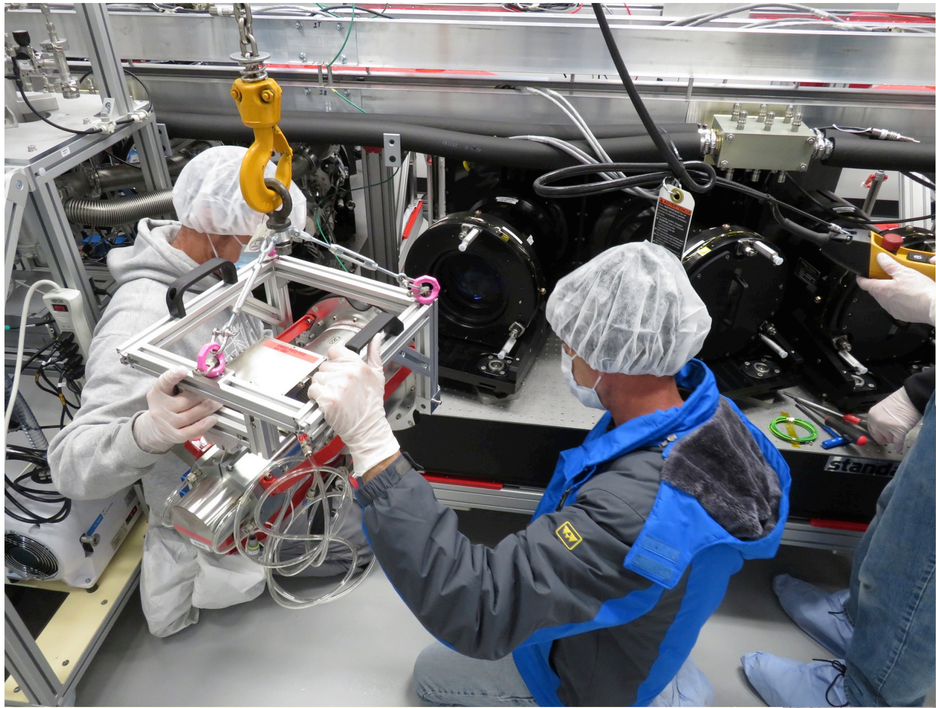

6 spectrographs installed

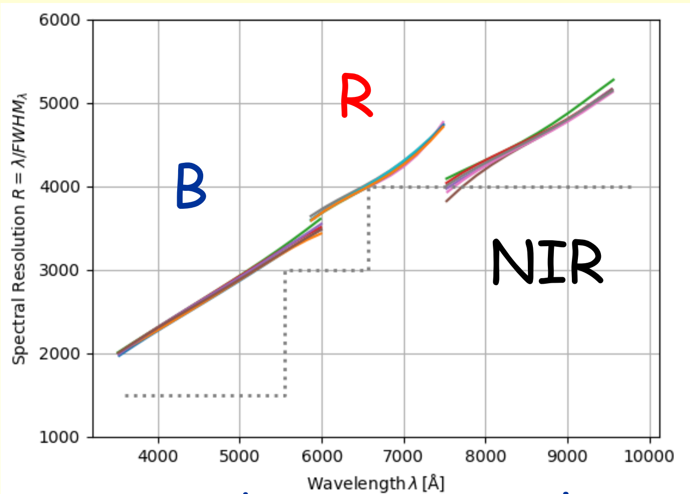

and operational

June 2019

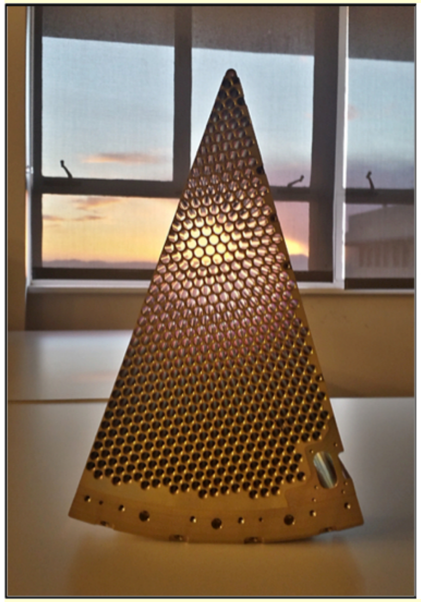
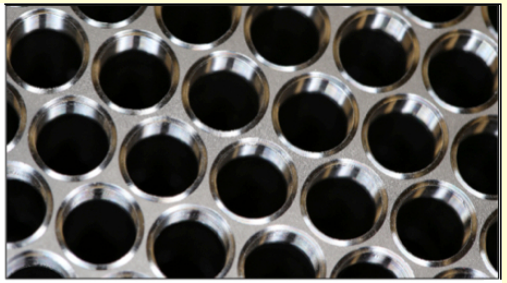
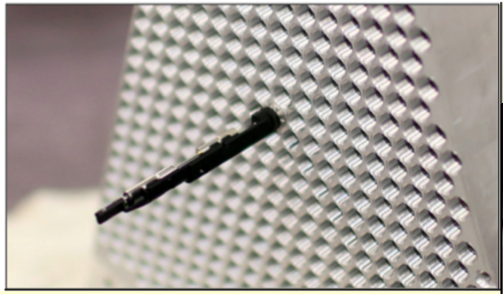

DESI focal plane

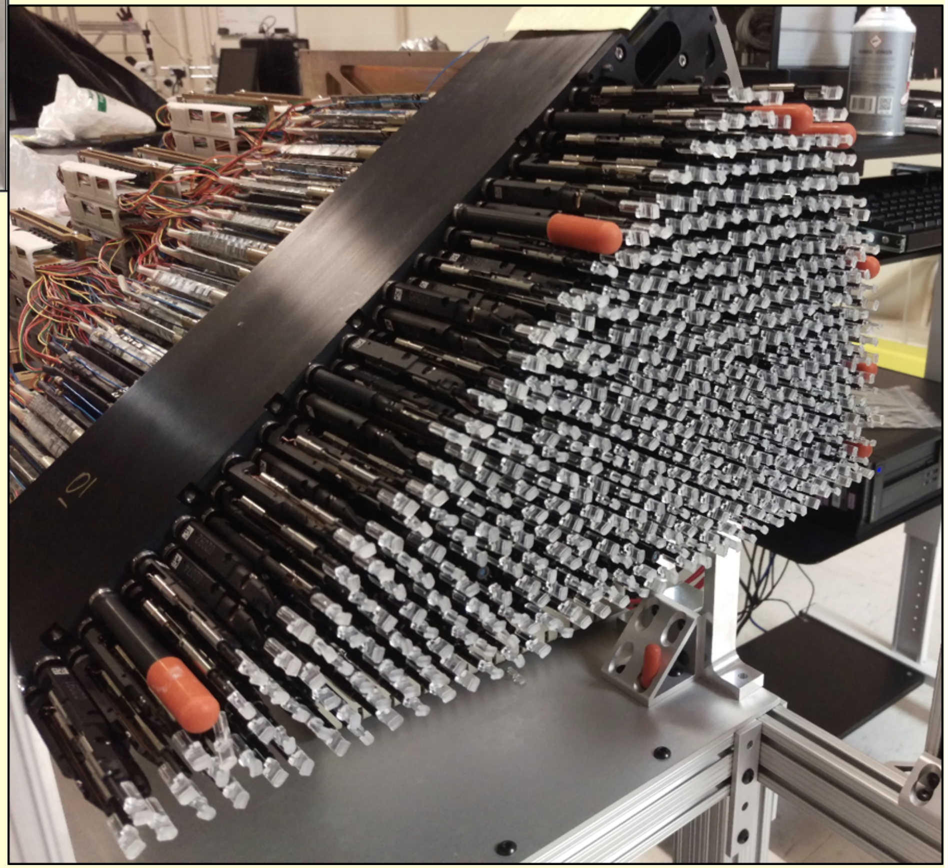

Focal Plane = 10 petals, each with 500 fiber-optic cables moved by robotic positioners

each fiber collects light from a separate sky object

DESI focal plane installation

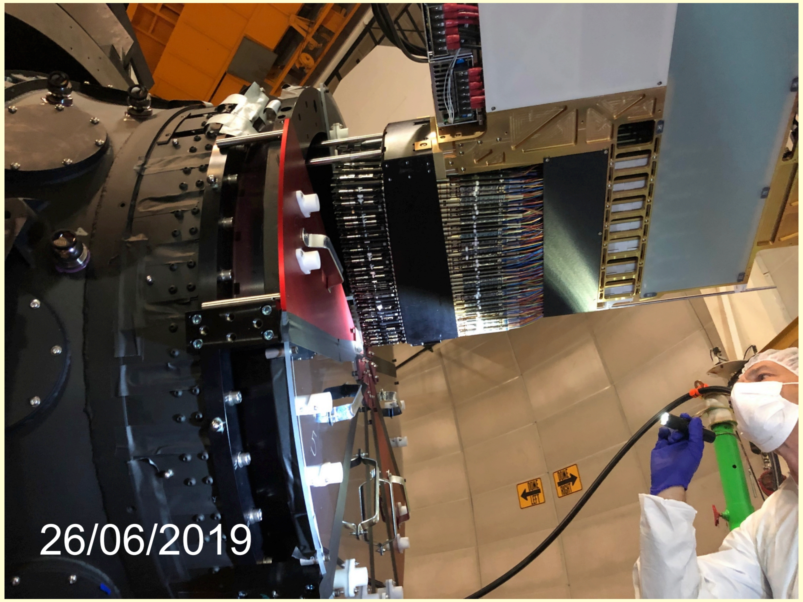

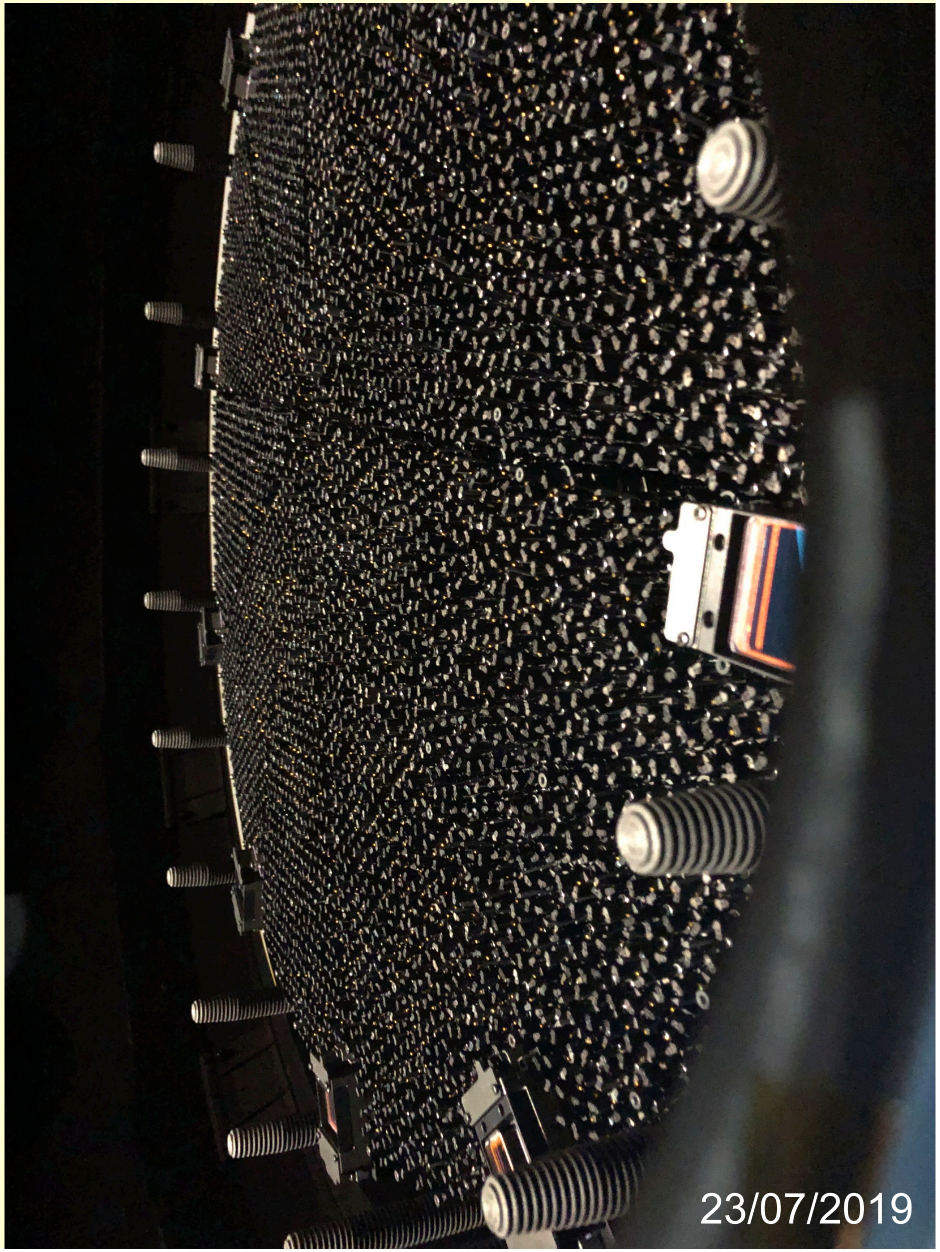

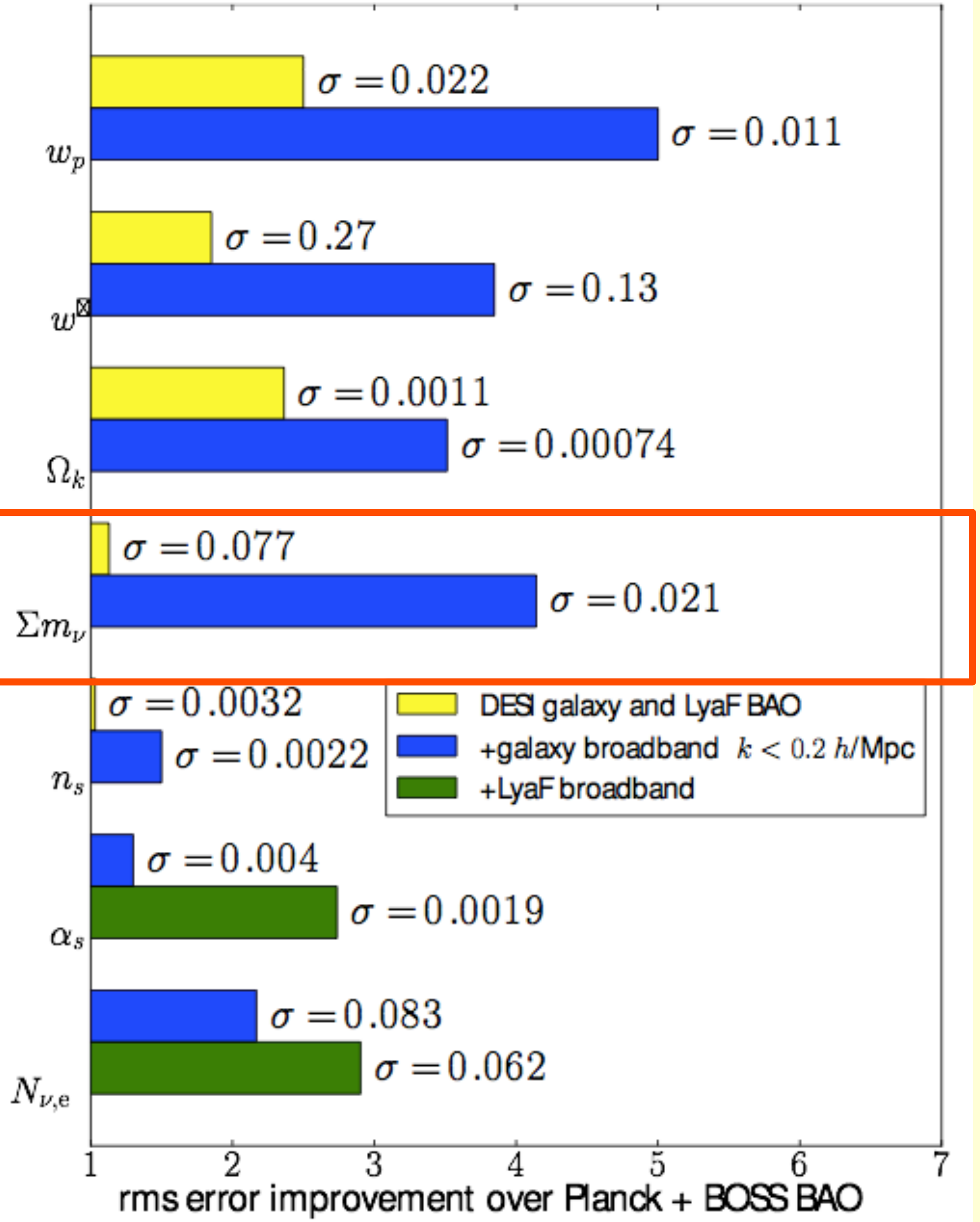

DESI prospects, arXiv:1611.00036